Since January 2020 Elsevier has created a COVID-19 resource centre with free information in English and Mandarin on the novel coronavirus COVID-19. The COVID-19 resource centre is hosted on Elsevier Connect, the company's public news and information website.

Computer Methods and Programs in Biomedicine 196 (2020) 105627

Contents lists available at ScienceDirect

Computer Methods and Programs in Biomedicine

journal homepage: www.elsevier.com/locate/cmpb

Computational fluid dynamics modelling of human upper airway: A review

W.M. Faizal[a,b], N.N.N. Ghazali[b], C.Y. Khor[a], Irfan Anjum Badruddin[c,d,*], M.Z. Zainon[b], Aznijar Ahmad Yazid[b], Norliza Binti Ibrahim[e], Roziana Mohd Razi[f]

[a] Department of Mechanical Engineering Technology, Faculty of Engineering Technology, University Malaysia Perlis, 02100 Padang Besar, Perlis, Malaysia
[b] Department of Mechanical Engineering, Faculty of Engineering, University of Malaya, 50603 Kuala Lumpur, Malaysia
[c] Research Center for Advanced Materials Science (RCAMS), King Khalid University, P.O. Box 9004, Abha, 61413, Asir, Kingdom Saudi Arabia
[d] Mechanical Engineering Department, College of Engineering, King Khalid University, PO Box 394, Abha, 61421, Kingdom of Saudi Arabia
[e] Department of Oral and Maxillofacial Clinical Science, Faculty of Dentistry, University of Malaya, 50603, Kuala Lumpur, Malaysia
[f] Department of Paediatric Dentistry and Orthodontics, Faculty of Dentistry, University of Malaya, 50603, Kuala Lumpur, Malaysia

ARTICLE INFO

Article history:
Received 14 April 2020
Accepted 21 June 2020

Keywords:
Human Upper Airway (HUA)
Computational Fluid Dynamics (CFD)
Fluid-structure Interaction (FSI)

ABSTRACT

Background and objective: Human upper airway (HUA) has been widely investigated by many researchers covering various aspects, such as the effects of geometrical parameters on the pressure, velocity and airflow characteristics. Clinically significant obstruction can develop anywhere throughout the upper airway, leading to asphyxia and death; this is where recognition and treatment are essential and lifesaving. The availability of advanced computer, either hardware or software, and rapid development in numerical method have encouraged researchers to simulate the airflow characteristics and properties of HUA by using various patient conditions at different ranges of geometry and operating conditions. Computational fluid dynamics (CFD) has emerged as an efficient alternative tool to understand the airflow of HUA and in preparing patients to undergo surgery. The main objective of this article is to review the literature that deals with the CFD approach and modeling in analyzing HUA.

Methods: This review article discusses the experimental and computational methods in the study of HUA. The discussion includes computational fluid dynamics approach and steps involved in the modeling used to investigate the flow characteristics of HUA. From inception to May 2020, databases of PubMed, Embase, Scopus, the Cochrane Library, BioMed Central, and Web of Science have been utilized to conduct a thorough investigation of the literature. There had been no language restrictions in publication and study design of the database searches. A total of 117 articles relevant to the topic under investigation were thoroughly and critically reviewed to give a clear information about the subject. The article summarizes the review in the form of method of studying the HUA, CFD approach in HUA, and the application of CFD for predicting HUA obstacle, including the type of CFD commercial software are used in this research area.

Results: This review found that the human upper airway was well studied through the application of computational fluid dynamics, which had considerably enhanced the understanding of flow in HUA. In addition, it assisted in making strategic and reasonable decision regarding the adoption of treatment methods in clinical settings. The literature suggests that most studies were related to HUA simulation that considerably focused on the aspects of fluid dynamics. However, there is a literature gap in obtaining information on the effects of fluid-structure interaction (FSI). The application of FSI in HUA is still limited in the literature; as such, this could be a potential area for future researchers. Furthermore, majority of researchers present the findings of their work through the mechanism of airflow, such as that of velocity, pressure, and shear stress. This includes the use of Navier–Stokes equation via CFD to help visualize the actual mechanism of the airflow. The above-mentioned technique expresses the turbulent

* Corresponding author.
E-mail addresses: nik_nazri@um.edu.my (N.N.N. Ghazali), magami.irfan@gmail.com (I.A. Badruddin).

https://doi.org/10.1016/j.cmpb.2020.105627

kinetic energy (TKE) in its result to demonstrate the real mechanism of the airflow. Apart from that, key result such as wall shear stress (WSS) can be revealed via turbulent kinetic energy (TKE) and turbulent energy dissipation (TED), where it can be suggestive of wall injury and collapsibility tissue to the HUA.

1. Introduction

Breathing, known as ventilation, is the process of taking air into and expelling it from the lungs, often by consuming oxygen and discharging carbon dioxide from the lungs. The respiratory system comprises the nose and mouth, and all the way through the respiratory tract: airways and lungs. Lungs are the main organs of the respiratory system, in which it works to exchange oxygen and carbon dioxide during breathing. The nose and mouth are used for breathing, where the air would then enter the respiratory system, along the throat (pharynx), and across the voice box (larynx). Food and drink are blocked from entering the airways during swallowing because the passage to the larynx is lined with a small flap of tissue called the epiglottis, which will spontaneously close upon swallowing. The upper airway is situated at the lower end of the trachea, which refers to the airway segment within the nose or mouth and the main carina. The segment between the trachea and the mainstem bronchi is the central airways. The lower conducting airways, such as the main, lobar, and segmental bronchi, are different from the upper airway in a sense that the latter has no collateral ventilation. As such, any obstruction of the upper airway or central airways can be fatal, be it an acute obstruction (occurrence within minutes) or a chronic one (development in weeks or months). Asphyxia and fatality may be resulted from any clinically significant obstruction that take place along the site of the upper airway; this is where recognition and treatment can be lifesaving. The upper airways are segregated into four sections: the nose (functional during nasopharyngeal breathing) and the mouth (functional during oropharyngeal breathing), the pharynx, the larynx, and the trachea. Due to the parallel anatomic arrangement of the nose and the mouth, they seldom become an upper airway obstruction, unless in the event of massive facial trauma. Central airway obstruction is a branch of the upper airway obstruction, which includes trachea and mainstem bronchi.

In recent years, the study of human upper airway (HUA) has become one of the interesting research areas. Some studies were focused on the flow characteristics, computer modeling, and fluid-structure interaction between the airflow and the soft tissue of the upper airway. Human upper airway plays a crucial role in delivering the inhaled air from the nasal passages to the lungs, which is a part of the body's breathing mechanism. The unique anatomical structure and functional properties of the soft tissue of the upper airways (e.g., mucosa, cartilages, and neural and lymphatic tissues) significantly influence the airflow characteristics and have a crucial effect to the conduction of air to the lower airways. Fig. 1 shows the anatomy of human upper airway, which begins with the nasal cavity and continues over the nasopharynx and oropharynx to the larynx [1]. The function of the upper airway is not limited to only deliver air to the lung, but it ensures normal phonation, digestion, humidification, olfaction, and warming of inspired air [2]. Therefore, the better understanding of human upper airway may enhance the clinical application of anatomical structure and improve the physiological knowledge of the respiratory system for a medical practitioner.

An abnormal breathing during sleep can be classified in various forms and conditions, such as sleep apnea, sleep-disordered breathing (SDB), sleep apnea-hypopnea syndrome (SAHS), and sleep-related breathing disorder (SRBD), all of which arise from different etiologies [3]. Many researchers are concerned about the importance of abnormal breathing during sleep, to which they have proposed different efficient methods to detect or monitor the breathing performance of the patient [4]. On top of that, the scholars have proposed other efficient ways to treat the abnormal sleep breathing patient via skeletal surgical approach [5], volumetric tongue reduction [6], and using oral appliances to improve the their sleep breathing experience [7,8].

The primary physiological objective of sleep is the patency of the upper airway. The relaxation of throat muscle narrows the airway and causes the failure of upper airway patency, which leads to the obstructive sleep apnea (OSA) and its sequelae [9]. Moreover, the protective upper airway is weak during sleep and the relaxation of the soft tissues can easily lead to the upper airway collapse [10]. OSA can be classified as a multifactorial disease, which involves a complex interplay of the upper airway anatomy, alone and/or a combination of neuromuscular control mechanism with other pathophysiologic factors (e.g., respiratory arousal threshold and loop gain) [11]. Dynamic tongue movement and tongue thickness may impair the respiratory control of an OSA patient. The factors that contribute to the OSA vary individually. Thus, an understanding of the OSA mechanism is important to achieve the goal of individualized and targeted therapy for patients [12]. However, some restrictions such as lack of information on the flow behavior and upper airway collapse can result in only 50% operation success rate [13]. Therefore, the knowledge and understanding of the flow properties of upper airway are practically important for medical practitioners and surgeons to accurately locate the obstruction in OSA patients [14,15].

Surgical correction of OSA syndrome is one of the alternative methods to tackle the obstruction of the upper airway [16]. The understanding of a three-dimensional (3D) airway anatomy is crucial for the surgical correction of OSA because it involves a number of parameters such as internal airflow velocity, wall shear stress, and pressure drop [17]. The advanced cone-beam com-

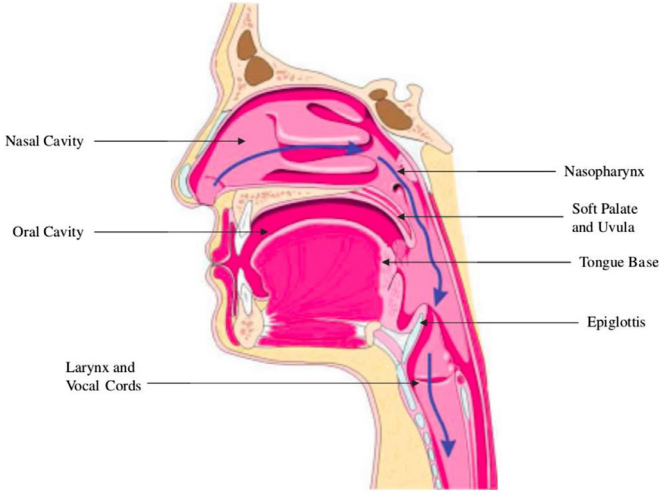

Fig. 1. The human upper airway is described as the area of airway between the nose (nasal cavity) and the mouth (oral cavity), and the main carina at the lower end of the trachea [5].

puted tomography (CBCT) scan and automated computer analysis were used to facilitate the visualization of the 3D upper airway in identifying the abnormal airway condition and their response to surgery. Besides that, preoperative studies provide knowledge and information on specific airway obstruction, which can grant precise surgical treatment for OSA patients by focusing on the specific region [18]. For example, 75% to 100% success rate of operation for maxillomandibular advancement (MMA) was reported in the surgical correction of OSA syndrome [19].

In recent years, the computational fluid dynamics (CFD) method has been widely employed to analyze the airflow in both healthy and diseased human conducting airways [20]. Most studies have focused on the pollutant transport and drug delivery in respiratory systems, whereas others focused on sleep-disordered breathing [21]. During breathing, the airflow characteristics through the human respiratory tract are very complex. The airflow can be in the laminar, transitional, or turbulent condition. The geometry and boundary conditions are the main factors that greatly affect the airflow in human respiratory tracts [22]. Therefore, these factors must be considered in the CFD study of respiratory flow. Sometimes, the simplified airway geometries are considered in the CFD analysis due to the limitations of computing memory and time. With the advancements in medical imaging techniques, unique and realistic geometries of the respiratory tract can be reconstructed from the scanned images, to which they can be converted into a CFD model; this also applies for both extra- and intra-thoracic airways [23].

The CFD analysis is able to provide clear visualization and its results can cover the lack of information from experiments such as the flow properties and flow pattern generated inside the human upper airway [24]. Moreover, the rapid development of new computational and numerical methods using powerful hardware can now shorten the computation time, allowing researchers to study the critical airflow of the upper airway prior to conducting the surgery [25]. This makes CFD a vital and useful tool for predicting the various flow properties in the human upper airway by computationally solving flow equations [26]. Thus, this review article focuses on the challenges that arise in analyzing the airway mechanisms via CFD approach, and critical process, including modeling and its mathematical background that are related to the study of the human upper airway (HUA). In addition, the various steps involved (i.e., preprocessing and post-processing) in solving the CFD analysis are investigated. Lastly, the application of CFD method in the analysis of the human upper airway, which has been carried out by previous scholars, is also discussed in this article.

2. Diseases associated with human breathing

As mentioned beforehand, the upper and central airways are the parts of a human breathing airway. These airways can be afflicted by respiratory diseases, which can distress or impair organs and structures that are related to breathing, such as the nasal cavities, the pharynx (also known as throat), the larynx, the trachea (or windpipe), the bronchi and bronchioles, the tissues of the lungs, and the respiratory muscles of the chest cage. There are many causes of respiratory illnesses and diseases; some of them are through infection, smoking of tobacco or breathing in secondhand tobacco smoke, asbestos, radon, as well as various types of air pollution. Asthma, chronic obstructive pulmonary disease (COPD), pneumonia, pulmonary fibrosis, lung cancer [27], and the newest pandemic-causing virus, COVID-19 coronavirus [32], are some examples of respiratory diseases. With regard to the human upper airway, an acute upper airway obstruction (UAO) occurs when there is a blockage in one's upper breathing passages. Since the trachea, larynx (voice box), and throat make up the upper airway of the respiratory system, a blockage in the airway may prevent the body from having sufficient oxygen uptake. Some types of breathing-related sleep disorder are related to a range of breathing abnormalities, from chronic or habitual snoring to upper airway resistance syndrome (UARS) and frank obstructive sleep apnea (OSA), and in certain circumstances, to obesity hypoventilation syndrome (OHS). On the other hand, computational fluid dynamics (CFD) is a computer-based software used to simulate the fluid movement. Some benefits of adopting the CFD method as opposed to other fluid mechanics analysis methods are that its significant cost and time savings, capability of analyzing extremely complex systems or conditions through experimental simulation (for instance, the case of airways), as well as a nearly unlimited level of detail. This review paper demonstrates that there is a broad application of CFD in the analysis of diseases, even those related to the respiratory system, where a better understanding of the airways mechanism during breathing can be attained. Table 1 outlines the author and the respective disease that was analyzed via CFD.

3. Challenges in analyzing airway mechanism

The airflow in the human upper airway is complex and time dependent. The airflow undergoes transition from laminar to turbulent, and vice versa within a second [35]. The complex geometry of the human upper airway results in curve streamlines, recirculation or vortex regions, secondary flow, and jet flow. In order to study the human upper airway, the laminar-turbulent transition flow with complex geometry can be analyzed via experimental and computational approaches. Both methods require a similar first approach, which is the preparation of the geometry model for a human upper airway [36]. The geometry model can be generated from the images captured or scanned from the medical imaging process, such as CT scan and MRI, among others [37].

3.1. Experimental methods

In the experimental method, a prototype of the human upper airway is fabricated based on the unique geometry of the upper airway of a patient, and the experiments are performed on this physical prototype [38]. The prototype of the upper airway is typically fabricated according to the actual dimension or that in a scale model, such as reduced- or enlarged-scale model. The operating parameters are considered in the experiments to evaluate the velocity, pressure, and flow profile of an upper airway. Several factors, such as time and cost, are required for the study, as well as the availability of facility, and measurement device that needs to be taken into consideration in the experimental works [39]. Furthermore, other errors, such as measurement and human errors, may influence the accuracy of data collected from the upper airway experimental setup. Many scholars had performed experimental analysis on various upper airways from different patients to identify the accurate causes, and to propose the response for surgery and operation [40]. Pirnar et al. [41] investigated a clear physical interpretation by developing a simplified experimental system. The mechanical representation was employed to represent the human upper airway. They implemented the liquid lining effects in a fluid flow-structure interaction computational model, as shown in Fig. 2.

3.2. Computational methods

Computational fluid dynamics method is an alternative way of analyzing and solving a complicated fluid flow problem. Although the CFD is widely applied in the engineering field, it can also be an extremely powerful tool in the biomedical research field. CFD solves the governing equations of fluid flow while advances the

Table 1
Analysis of diseases associated with human breathing through CFD.

Author	Related disease	Summary
De Backer et al. [28]	Asthma	A number of 14 cases of patients with mild to moderately severe asthma had undergone the CT scan twice subsequent to adequate washout of the bronchodilators. The varying amounts of exhaled air during a force (i.e., ability to move the air out of the lungs) are assessed by the CT scan model and calculated via the CFD analysis.
Wenwen et al. [29]	Asthma	In the diagnosis of 4-year-old asthmatic children, a planar and symmetric model of airways were reviewed. The CFD was used to conduct numerical works on the airflow and particle deposition in the upper and lower conducting airways.
Yang et al. [30]	Chronic obstructive pulmonary disease (COPD)	The aim of this work was to evaluate the effect of inlet velocity profile on the flow features in blocked airways along the branches of a human lung. Evaluation of bifurcation flow in a human lung was deemed vital to give a better prediction on the particle deposition in drug therapy and inhalation toxicology. This is done through the use of fully 3D incompressible laminar Navier–Stokes equations and continuity equation, while the CFD solver was used to solve the unstructured tetrahedral meshes.
Ali et al.[31]	Respiratory disease (lung airways)	CFD and particle dynamics framework on a specific lung model of a patient were described under unsteady flow conditions, which can enhance the knowledge of particle transport and deposition in the airways. Essentially, this can be a useful guide for future targeted drug delivery studies.
Jinxiang et al. [32]	Respiratory obstructive diseases (bronchial tumor)	Potential sites of diseases were investigated in this work, where disease severity was determined to help formulate a targeted drug delivery plan for the treatment of the disease. CFD was employed to provide visualization of the unique lung structure in assessing the exhaled aerosol distribution. CFD is also sensitive to the varying airway structures.
Qingtao et al. [33]	Lung cancer	The changes in structural and functional of the tracheobronchial tree post-lobectomy was assessed via the CFD to depict the airflow characteristics of the wall pressure, airflow velocity, and lobar flow rate.
Long et al. [34]	Pulmonary fibrosis (lung disease)	The respiratory system was assessed through the use of CFD method and compared with the pulmonary acinus mechanics and functions in healthy.

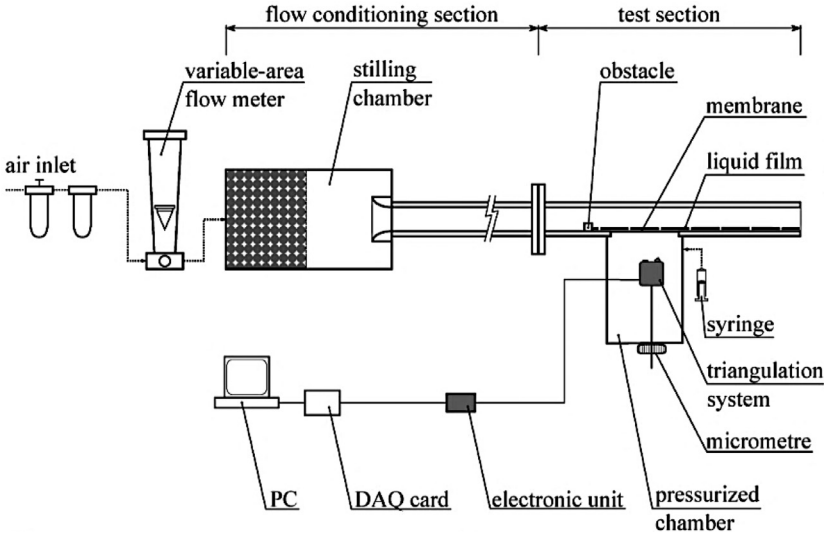

Fig. 2. Conceptual framework of fluid flow-structure interaction modeling. Experimental setup aims to assess the interaction between the unsteady airflow, liquid film, and compliant insert (e.g., silicone membrane) [41].

solution via space and time [42]. Fernández-Parra et al. [43] explored the air pressure and airflow resistance in the upper airway respiratory system and trachea of nine sedated and sternally recumbent dogs that have distinctive skull types. CFD was used to analyze the conduction of analysis via an inspiratory flow that is modified to the bodyweight of each dog. Ji et al. [44] demonstrated a detailed correlation among the flow and structure characteristics of the upper airways and airway collapsibility in obstructive sleep apnea, while the CFD was used to project possible collapsible sites along the upper airway. Numerous works have been done to study the fluid mechanism in human bodies. For instance, Ratchanon et al. [45] had performed CFD simulations according to the Euler-Euler approach to assess the airflow behavior upon an electrostatic charge of a full breathing cycle in the case of aerosol deposition in the trachea. In addition, Koullapis et al. [46] had studied the efficiency of computational fluid-particle dynamics approach for the prediction of deposition in a simplified approximation of the deep lung.

Moreover, the availability of computational resources for solving numerical algorithm also makes it possible to govern equations using a specific numerical method [47]. The combination of conventional coupled CFD-DEM model is also able to solve fluid-structure interaction (FSI) problems. The integration of a dynamic meshing approach allows the FSI simulation to resolve the flow structure surrounding the large free-moving object. Commercial software platform, such as ANSYS FLUENT, with user-defined functions (UDFs) are used to simulate the analysis due to its capability in handling complex geometries of the model and solving the dynamic meshing [48,49]. Recently, the FSI simulation analysis of the upper airway was adopted to explain the mechanism of pharyngeal collapse and snoring [50]. Various CFD commercial software tools use different discretization methods (e.g., finite difference, fi-

nite element, and finite volume methods) for solving the governing equations. ANSYS FLUENT is a popular software for CFD code, which has been widely used in the simulation and research of the human upper airway. In the CFD analysis, ANSYS FLUENT separates the analysis into three main stages, which are: (i) preprocessing, (ii) solver; and (iii) post-processing. However, to predict the flow accurately in the study of the upper airway, the selected numerical method must have the capability to simulate the low-Reynolds number turbulence model in a complex geometry [51]. The CFD model requires validation to ensure the reliability of the predicted results as reference.

3.3. Validation

Model validation is a very important step in any simulation analysis to ensure the models are performing as expected or mimics the real condition. Similarly, model validation in biomechanical modeling of the human upper airway with clinical data gains the confidence of users in utilizing the CFD computations. The rapid growth of interest in biomechanical modeling of the human upper airway since the 1990s has provided a better understanding and explanation of its physiology and pathophysiology. In the CFD model validation, the experimental data or clinical data benchmark is usually used to validate the simulation results [52,53]. The validated CFD model is expected to provide reliable results that are useful as reference for medical doctors in further understanding the problems of the human upper airway. Based on previous literatures, there are many ways to perform validation via the CFD model; for example, comparing previous results from other researches in terms of similar parameter. *In vitro* experiment, such as the studies of biological properties that are done in a test tube rather than in a human or animal, is also employed in the CFD model validation. Moreover, the mesh independence study is a popular technique to ensure the accuracy and consistency of the CFD model. The CFD model is expected to validate and provide reliable predictions when the convergence of the results is achieved in mesh independence study.

Chouly et al. [54] proposed the validation method of the numerical upper airway model through *in vitro* experiment, which mimics the section of the human upper airway at the lay-down position. Overall configuration and the dimensions of upper airway were conserved to maintain the realistic of the replica. The *in vitro* replica mimics the asymmetries of the upper airway geometry by using a rigid pipe and a removable flat plate. Rigid or latex with water was used to represent the tissue properties at the base of the tongue, in pathological conditions. The *in vitro* experimental setup is illustrated in Fig. 3, while Fig. 3a shows the morphology of the upper airway. Pressure sensors were used to record the pressure variation of the airflow at each time step. The wall deformation of latex was recorded by the digital camera, and the simulation results were compared and validated by the measurement results of the *in vitro* replica.

Verification and validation of CFD results are required to determine the degree of accuracy that represents the real case scenario. Zhao and Lieber [55] had carried out an experiment of a flow passing through a simplified symmetric bifurcation model without considering its unique features, as depicted in Fig. 4, where the Reynold's number considered was Re = ~2100. The distribution of axial velocity was plotted at different locations of 1, 3, 11, 15 in the *x-y* plane, and locations of 10 and 15 in *x-z* plane. This bifurcation model was then further validated by Mihai et al. [56] in their CFD pharyngeal airflow study. Various turbulence models (e.g., LES and RANS) were employed to simulate the turbulent airflow behavior in a bifurcation model. The simulation results were compared with Zhao and Lieber's experiment [55], as shown in Fig. 5. Comparing CFD results with available experimental data is a popular technique to validate the CFD model or analysis. A good agreement between the experimental and simulation results indicates the strong capability of CFD model to reflect the reality or real condition. CFD validation is not only limited to the results, but it is also applicable for the methodology. The CFD methodology is compared with the experimental flow data to ensure the airway has the similar conditions before it can be extended for parametric study using the same model [57,58]. Table 2 summarizes the differences between experimental and computational approaches for various applications.

4. CFD critical process

The mechanical properties of the upper airway are important to define the obstructive events in detail, such as the relaxation of the soft tissue during sleep [61]. A better understanding of the mechanism involved in the obstructive upper airway can be achieved via experimental and numerical studies [62]. A particular numerical simulation method, CFD, is the best approach to describe the mechanical properties in the upper airway, where it is popularly used by researchers to describe the obstacles in the upper airway. The first step to analyzing the upper airway requires the geometry model of the CFD simulation, which helps in visualizing and describing the airflow. The geometry model of the upper airway is usually created based on the MRI or CT scan images. The fluid domain of interest is identified and segmentation is subsequently carried out to further divide the domain in smaller segments, with the grids and elements; this is known as mesh generation in the fluid domain of interest. Rapid development and advancement of commercial software facilitates the mesh generation step via various popular software, such as ANSYS Workbench, ANSYS ICEM CFD, CFD-GEOM, Tgrid, and Gridgen.

4.1. Preprocessing

Preprocessing is the initial step of the CFD simulation analysis, comprising the identification of domain interest, creating a domain for the upper airway, and mesh generation on the domain. The preprocessing step is not limited to the study of upper airway, rather, it is also widely applied in the CFD analysis of various engineering problems. In this step, modeling goals, such as the initial assumptions of the airflow (e.g., steady and unsteady flow) and the model (e.g., laminar and turbulent), that are used to describe the airflow must be clear on the given problem of the upper airway. Moreover, the degree of accuracy, computation time, and simplification also needs to be considered in the initial step of the CFD simulation process. Essentially, the preprocessing step of the CFD analysis includes the following:

(i) Identifying the domain of interest:

Fig. 6 shows the schematic diagram of human upper airway in the anatomy of the nasal airway. The regions of the nasal airway were divided into nine different cross sections, and defined based on the nomenclature and magnitude of the airflow velocity [63]. The selection of specific section was considered according to the interest of the study.

(i) Creating an upper airway model of the domain:

The computational domain of the upper airway is typically created in a form of 2D and 3D models. The simplification of the upper airway model saves the computation time of the simulation. 2D approximation was considered for a continuous geometry, such as a model with chamfered rib and various simple shapes (e.g., circular, semicircular, rectangular, and triangular). However, the 3D approximations are usually

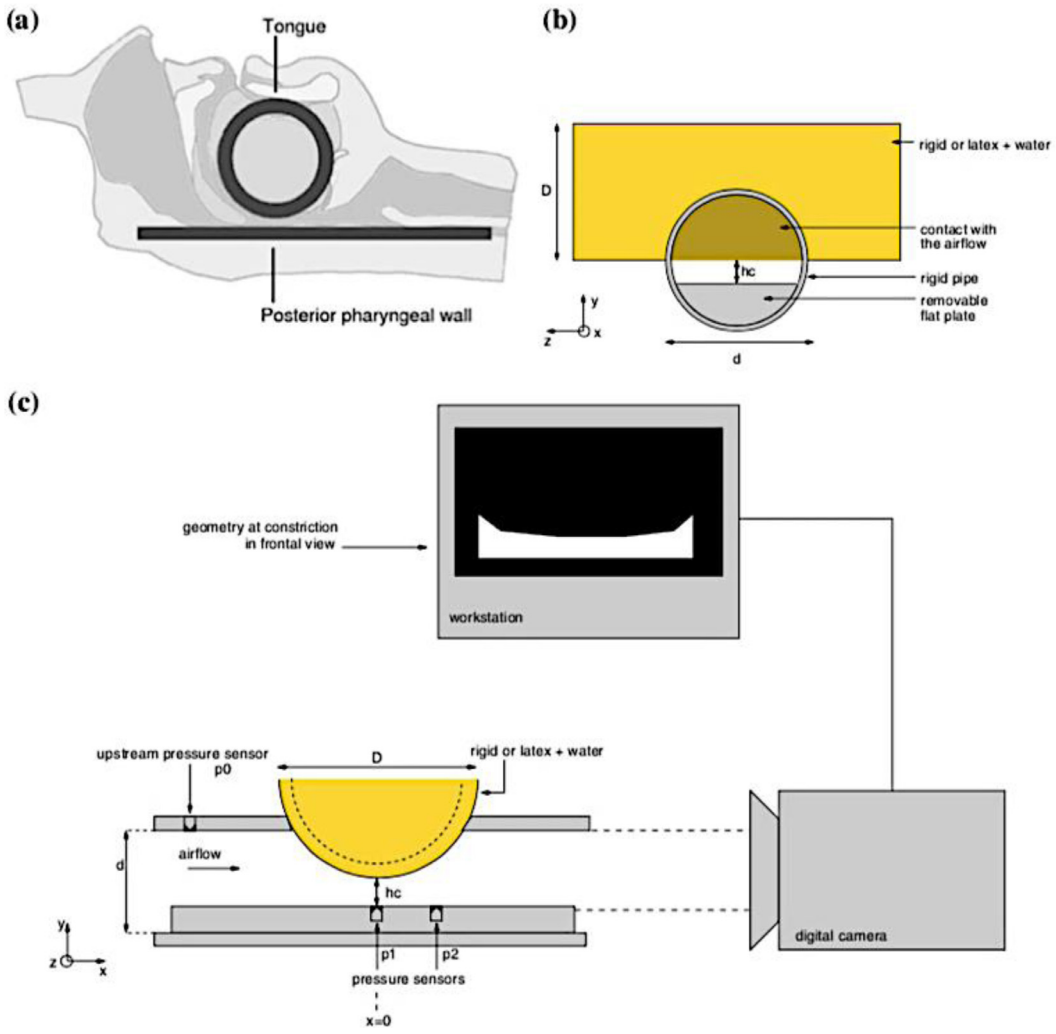

Fig. 3. (a) Morphology of the upper airway at sagittal view; (b) *In vitro* experimental setup from frontal view; and (c) Position of pressure sensor and digital camera in the experimental measurement of wall deformation [54].

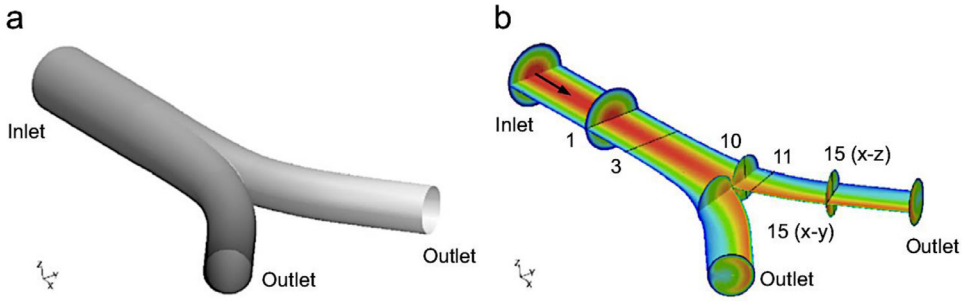

Fig. 4. (a) 3D computational domain of symmetric bifurcation model; and (b) distribution of axial velocity and locations of the extracted data line plots [55].

applied for complex geometries, such as arc-shaped roughness, as well as V- and Z-shaped rib roughness. Typically, the model of the upper airway is generated via a computer-aided design (CAD) software prior to defining the fluid (i.e., airway) or solid (i.e., soft tissue) domain of the model. In this step, the unnecessary features of the upper airway; such as shape, edge, and image noise that are created from the MRI or CT scan; will be removed. The simplification of the model can avoid complicated meshing or grid generation process, as illustrated in Fig. 7 [64]. The soft palate was assumed to be a flexible plate in the computational model, which separated the nasal and oral inlets. In the computational study of the upper airway, the model of the upper airway can be created using two approaches, either an approximation model or an accurate model.

(i) Mesh generation on the domain:

After the domain was created, the meshing or grid generation was performed to divide the airflow domain into a number of subdomains (elements or cells). In this step, the hexahedron and tetrahedron elements are usually used in the

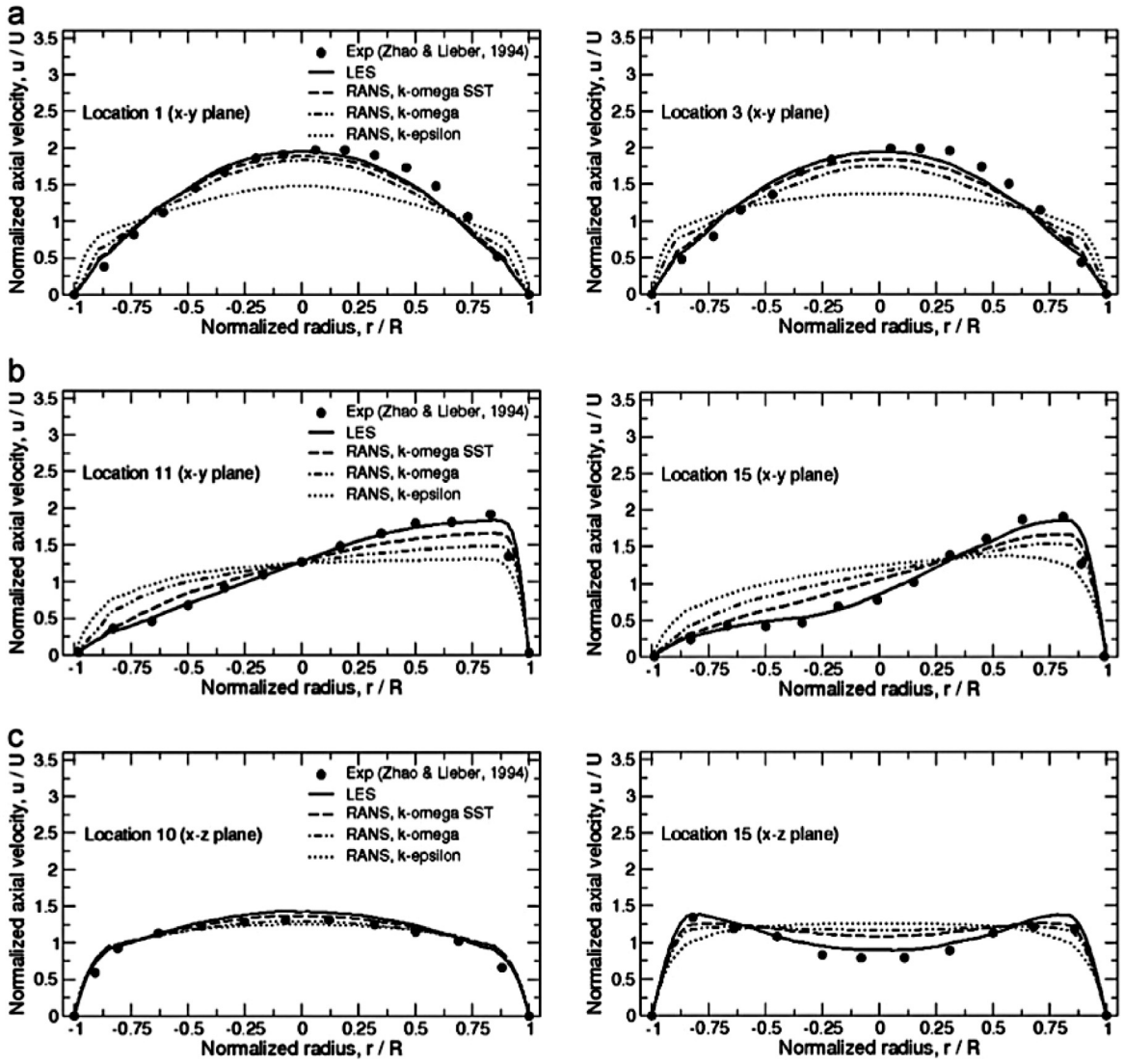

Fig. 5. Comparison of CFD result with that by Mihai et al. [59] and Zhao and Lieber [55].

Table 2
The differences between experimental and computational approaches [60].

Experimental	Computational
• Directly use the actual physical system in the real world. • Limited number of points for data measurement and time instants. • Higher cost associated with an experimental set up. • Limited range of problem and constraint of operating conditions. • Difficult to modify the experimental set up once manufactured or fabricated. • Require a large number of measuring instruments in the data collection. • Experimental works are not constrained by the complexity of the problem. • Slow, sequential and single purpose for the experimental work.	• Simplification is done on the physical system. • Simulation data in no limit in term of space and time. • Cost only for initial investment of commercial software. • Applicable for any range of problem virtually and for realistic operating conditions. • Computational model or domain can be modified easily here. • Various models and tools are available for calculation and data collection. • The computational approach is constrained by the build in mathematical models and require user defined functions, especially for complex system. • Fast computing, parallel and multi-purpose in computational approach.

3D domain. However, triangle and quadrilateral elements are generated in the 2D physical domain. The quality of meshing is important in the CFD simulation, as it has a significant effect on the convergence rate and accuracy of simulation results and computation time. Appropriate boundary conditions were also specified at the meshing elements of the domain. For example, five layers of prism cells were generated close to the wall region for better numerical stability and accuracy. Fig. 8 shows the boundary layer meshing in the study of the upper airway using a 2D nonuniform mesh [63]. The boundary layer meshing was expected to provide better stability during the simulation. Moreover,

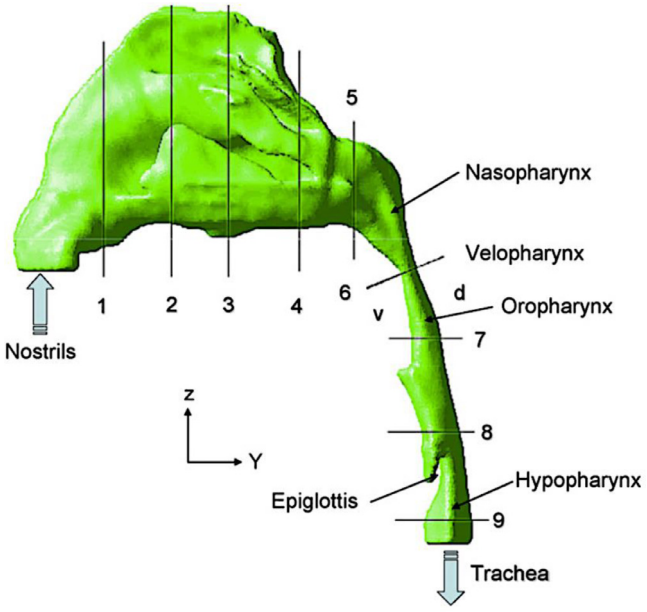

Fig. 6. Lateral view of segmented HUA of the nasal cavity and pharynx [63].

the grid independence test was required to determine the best number of cells or elements of a domain. The optimal number of elements reduces the computational resources, such as computation time while providing accurate predictions of the airflow through the simulation. In the grid independence test, different numbers of elements were considered for the domain, as shown in Fig. 9 [65]. Once the elements had achieved the optimal number, the further increase in the elements had less than 1% of variation in the result. Thus, the step to determine the optimal number of elements for a domain is necessary to obtain reliable and accurate CFD results.

In an upper airway analysis, creating an upper airway model of the domain is the most crucial step due to the complexity of human body anatomy (i.e., airway geometry). The simplification of the model is usually considered in the CFD simulation due to the above-mentioned complex and unique airway geometry. Today, with the advanced software, the complex geometry of the human upper airway is able to be recreated into a computational domain, keeping all unique features of the upper airway intact [66]. This provides a realistic model and accurate visualization of the airflow in the study of the upper airway. It was reported that detailed explanation of these upper airway geometries had been used in both experimental and simulation investigations [67].

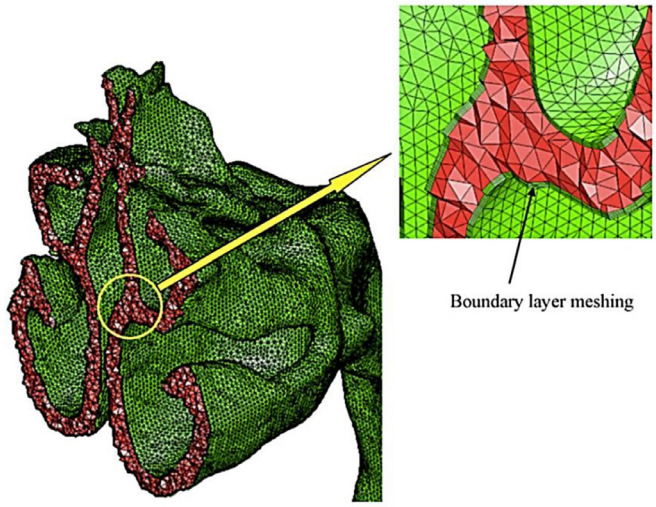

Fig. 8. Boundary layer meshing of the human upper airway [63].

4.1.1. Approximate model of the upper airway

Simplification of the model while creating a fluid domain for the model is common in CFD analysis. The simplified model is also known as an approximate model, which is usually simplified in terms of its dimension, cross sections, and shapes of the upper airway. Complex geometry leads to difficulties in the mesh generation and consumes high computation time due to the increased number of elements. Therefore, most of the previous studies of upper airway had simplified the geometric model in their simulation analysis [68]. The simplified model reduces the computation time, efforts, and eases the analysis, but compromises the accuracy of the CFD results. In the simplified model, assumptions are made to reduce the complexity of the airflow mechanism, such as a reverse flow in the airway.

Fig. 6 shows the geometries of peripheral airways in three dimensions. The simplified airways (i.e., CAD model) were constructed using a mechanical modeling software, AutoCAD 2012, to investigate the human tidal breathing [69]. The unique shape of airways was simplified, where it was assumed to be a smooth cylindrical airway. Normal and obstructive airways were varied by the diameter of the cylindrical airways, while the airflow characteristics were compared for different obstructions, as depicted in Fig. 6.

On the other hand, the upper airways were simplified into a 2D model to simulate the fluid-structure interaction (FSI) phenomenon of the soft palate in the pharynx using more than one turbulent model as a solver [70]. The multi-block structured grid was applied to the 2D model to represent the simplified geome-

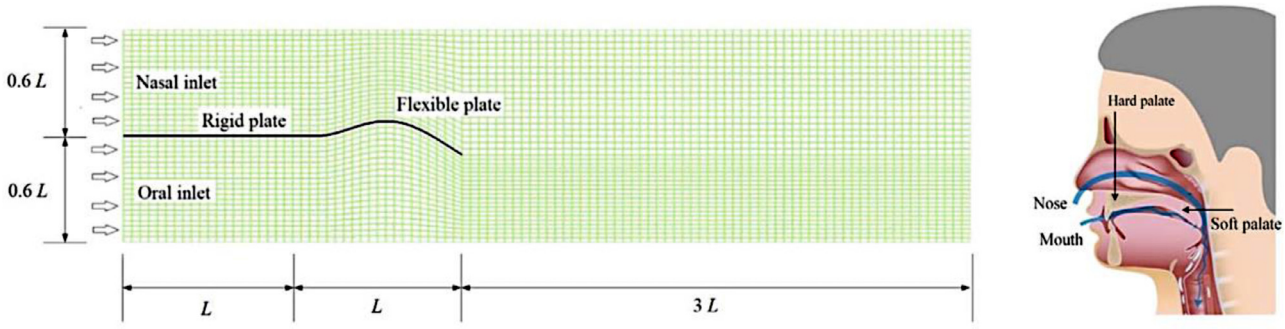

Fig. 7. Simplification of model on the possibility of preventing complicated meshing or grid generation process through a 2D-computational domain of a human upper airway [64].

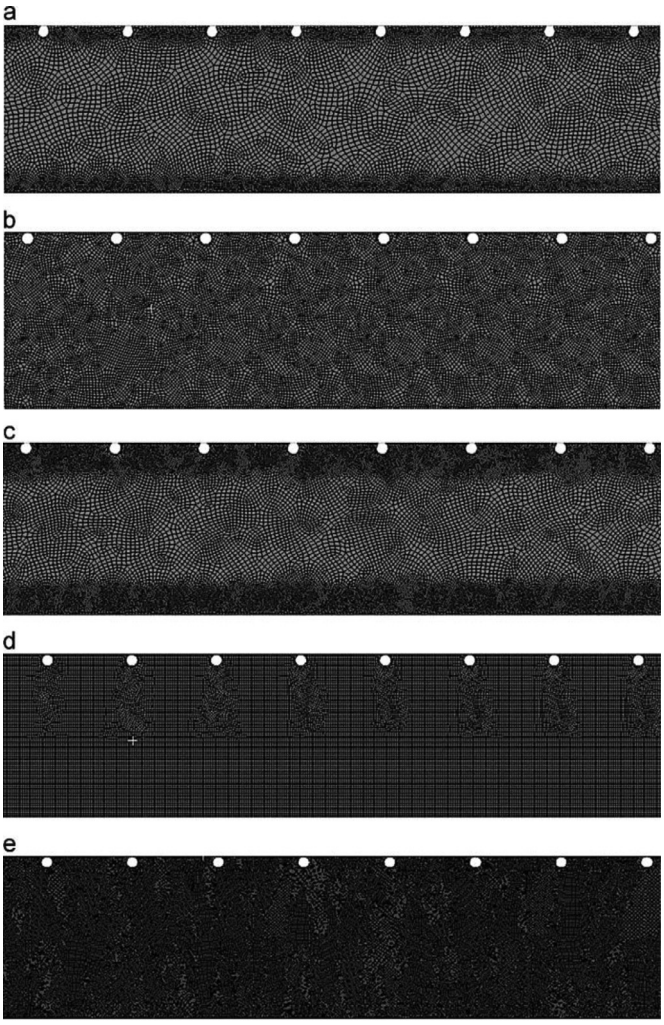

Fig. 9. Grid independence study for a domain with: (a) 103k; (b) 118k; (c) 137k; (d) 162k; and (e) 198k number of cells [65].

try (in rectangular) of the upper airways (Fig. 11) [64]. The curved region in Sections 3 and 4 represent the soft tissue or palate. Analysis of the simplified model is able to provide a better understanding of the OSA mechanism and snoring during sleep by considering the compressible viscous flow in the simulation [71].

4.1.2. Accurate model of the upper airway

An accurate model of the upper airway gives more reliable and precise results compared with that given by a simplified model. Medical imaging techniques (e.g., magnetic resonance imaging, MRI; and computed tomography, CT) help to construct the accurate model of the upper airway by keeping intact its unique feature of the patient [72]. The medical images captured from the CT, high-resolution computed tomography (HRCT), and MRI are imported and processed by the image processing software (e.g., 3D-Doctor, Mimics, and 3D Slicer) before the computational domain is created [73]. Fig. 12 depicts the typical steps to construct an accurate model of the upper airway, as well as that of other models (e.g., bone and tissue) [74]. The CT scan data were chosen for the image processing because they have a good contrast between bones and soft tissues compared with the MRI data. The volumetric data was constructed in the image processing step, while the Gaussian filters and edge detection were applied to remove the image noise. The specific region of bone is identified in this step, while the segmentation step separates the details of the bony structures. For example, the ligaments, tissues, cartilages, and bony structures, such as tibia and femur, are identified and defined in the image via a region-growing algorithm that is typically built in the algorithm of the commercial software. The defined regions were then created to form a profile series. Then, the detailed model (i.e., accurate model) was generated and meshed based on the profile series.

To generate an accurate model, the basic element used in generating the model is voxels. A voxel represents a value on a regular grid in three-dimensional space. Voxels of the tissue with fixed dimensions provide the coordinates and some attributes that characterize the position of the tissue. From the voxels, the surface of the model is then generated using the graphic rendering technique. The marching cubes algorithm is applied to extract the polygons from the volumetric data. The boundary voxels and surface triangulation are generated to represent the 3D object [75]. Finally, the vessel reconstruction process/meshing step is carried out to discretize the complex model into finite volumes or finite elements. Smaller volumes or elements are generated to resolve the complex flow in the accurate model. Apart from that, the specific region of the elements is used to define the boundary condition to compute the inlet velocity. The optimal number of meshing elements can be determined from the study of grid sensitivity to ensure the accuracy of the model.

Furthermore, the medical scan images (e.g., MRI dan CT scan) can be used to construct a 3D plastic model via the rapid prototyping (RP) technique. These medical images are converted into an STL file format and exported to the RP software. With the aid of the 3D plastic model, the airflow motion was studied by Chengyu et al. [76] through particle image velocimetry (PIV) method. Particle deposition in the oral airways can be observed in the PIV experiment. In their study, four different geometrical models of the upper airway were considered to investigate the geometrical effect on particle transport and airflow profile. A rapid prototype model was used in the study of turbulent flow of airways due to its cyclic and steady flow condition.

4.2. Solver of turbulence model

In a CFD simulation, the selection of flow model is crucial to simulate the mean flow characteristics that could represent the real flow condition. The selection of flow model is dependent on the applications and nature of the problem. The CFD consists of six turbulence models, which can be categorized into three main models: Reynolds-averaged Navier–Stokes (RANS), large-eddy simulation (LES), and direct numerical simulation (DNS). The RANS model is suitable for statistically steady solutions, in which it can solve the time-averaged Navier–Stokes equations for the flow variables. All turbulent motions of the flow are modeled in the simulation. The LES approach solves the filtered Navier–Stokes equations only in large-scale flow variables; the smaller vortices are not directly predicted. In DNS method, the model may be involved with finite computational elements. Meanwhile, DNS solves the full, unsteady Navier–Stokes equations to resolve the whole spectrum of the turbulent scales, where the prediction of turbulent flow is accurate but time consuming. A computation time-efficient method is very important, and it has always been considered as one of the criteria needed to obtain credible CFD results within a reasonable research timeframe. Thus, a two-equation RANS model, which is the standard k–ε (SKE) model, is preferred in the simulation study of the human upper airway [77].

Three turbulence models were compared with previous studies, which are realizable k–ε (RKE) model [78], the k–ω turbulence model [79], and its shear stress transport (SST) variant, k–ω SST [80]. Menter et al. [81] and Langtry et al. [82] had developed the four-equation transition SST model, which is more demanding compared with the two-equation model. Different models

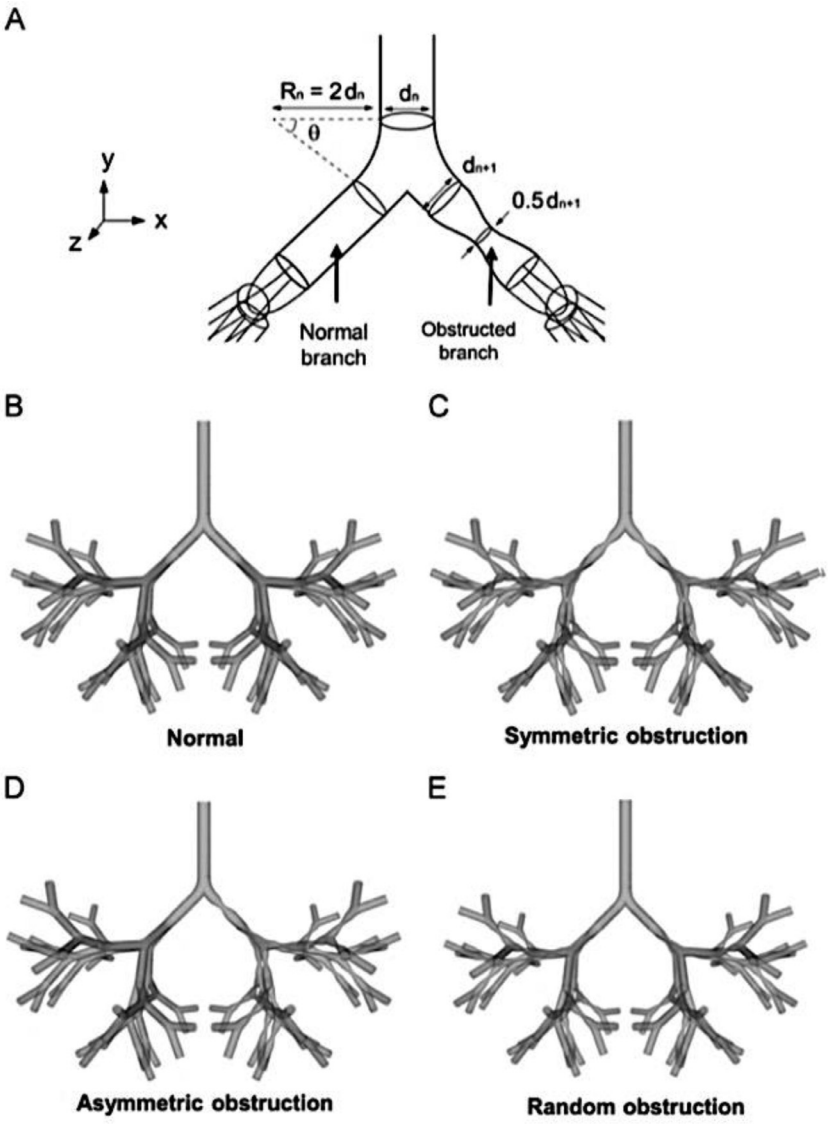

Fig. 10. Three-dimensional (3D) geometries of peripheral airways using AutoCAD 2012 [69].

have its own wall mesh treatment and mesh resolution, as shown in Fig. 13 [83]. The wall functions are typically employed in cases where a flow separation is not to be expected. Distance from the wall to the adjacent layer (y_p) is different for k–ε and k–ω models. Therefore, the dimensionless wall distance (y^+) is applied to assess the mesh resolution near the wall, as defined in Eq. (1):

$$y^+ = \frac{u_\tau * y_p}{\nu} \tag{1}$$

where, u_τ is the friction velocity based on wall shear stress and air density; and ν is the kinematic viscosity.

Direct numerical simulation (DNS) is one of the solvers in a computational fluid dynamics method that solves the Navier–Stokes equations numerically by considering the range of spatial and temporal scales of turbulence. In the DNS method, the model is in three dimensional, and the solution is time dependent. A few studies have employed the DNS method to investigate the compressibility of velocity transformations [84], droplet condensation [85], vortex shedding [86], and hydrodynamic forces in the cylinder [87]. However, only a limited number of geometrically simple flows were simulated via the DNS method; for instance, the flow over a flat plate or flow in a channel. Due to the complexity of the transport equation, additional computer programming is required, and this involves a huge amount of computation time during the simulation process. Therefore, the issues in any CFD simulation are always concerned with the numerical accuracy, convergence, solution stability, and correctness of the boundary conditions settings [88]. To visualize the detailed picture of the turbulent flow around a boundary layer, the three-dimensional model must be meshed with fine grids that will allow the equations to resolve the individual eddies or vortices. The grid size may be as small as between the range of 30 to 100 μm for a low viscosity fluid. For a transient flow analysis, a small-time step size (e.g., 0.001–0.01 s) must be applied to capture the unsteady characteristics of the turbulent flow. Because the fluctuation frequency raises when the Reynolds number is increased, the computing requirements become extensive for high Reynolds number flow. Computing facilities, such as great data storage capacity and high performance of computer, are important to facilitate the simulation process and shorten the computation time. Therefore, the DNS method is appropriate only for the moderate levels of turbulence simulation, where it is recommended for an ideal flow condition that cannot be developed in an experimental work [89].

Large-eddy simulation (LES) is an alternative solver to compute the flow field, which involves large vortices in the turbulent

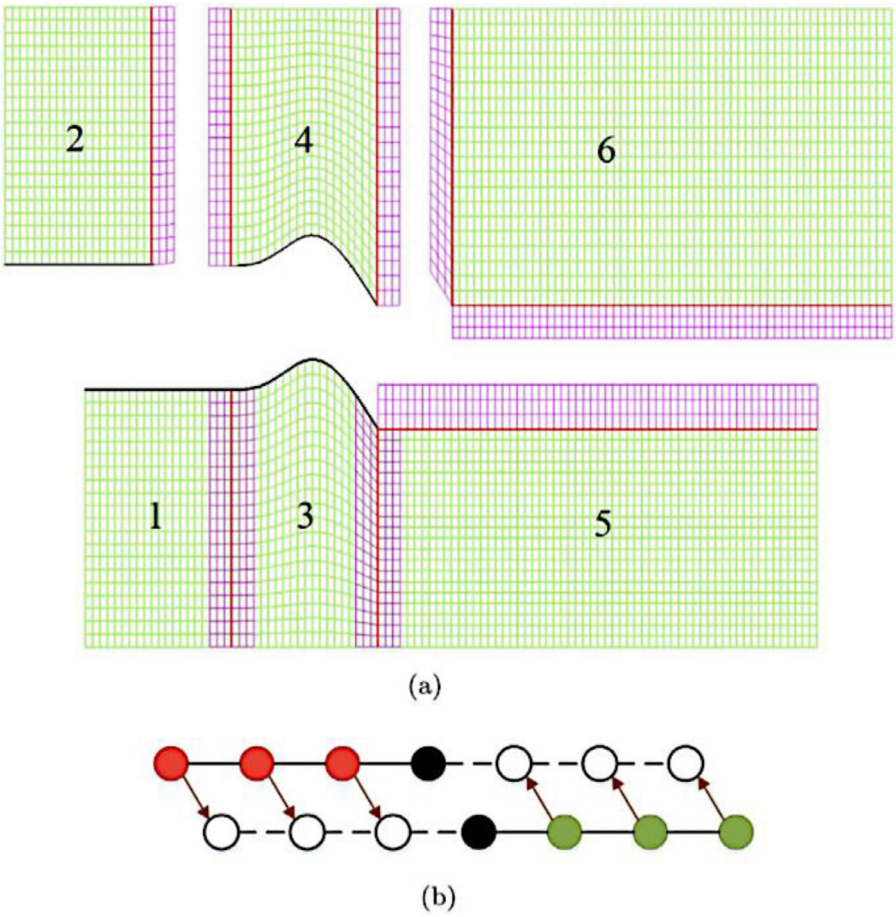

Fig. 11. Simplified geometry of the upper airways using a multi-block topology: (a) block-structure topology; and (b) points overlapping along a line [64].

flow analysis. Using this solver, the large eddy of the turbulent flow is tractable, while the small eddies are modeled. LES directly resolves the turbulence and the filtered Navier–Stokes equations in the simulation. Filtering is performed via the time-dependent Navier–Stokes equations, where the flow eddies are filtered out depending on the scales. The filtering in LES model uses a very similar equation for the RANS model in solving the momentum and energy equation for a compressible flow. Additional terms are introduced for approximation modeling, such as the subgrid-scale turbulent stresses and heat fluxes. These terms are used to create the close loop in the subgrid-scale models. The interconnection of different components in LES induces challenges in the application of LES modeling [90]. However, the LES has proven to be effective by producing astonishing results in solving industrial problems that deal with turbulent characteristics, in which it can overcome the constraints of RANS or unsteady RANS (URANS) models. The cost of application of an LES solver is less expensive compared with that of DNS, but the computational resources and efforts needed are too large for most practical or industrial applications. These efforts include the transition process of RANS to LES model, which accounts for implementation issues, such as the selection of filtering, near-wall treatment, and closure modeling [91].

A turbulent flow can be involved in various scales and combination of different flow mixtures or phases. There are different turbulence models that have been applied in simulation; for instance, the DNS is applicable for all scales, while the LES is for the larger scales of grid-imposed filter. Apart from that, the very-large eddy simulation and detached eddy simulation (V-LES and DES) are suitable for subscale variants. Reynolds-averaged Navier–Stokes equations (RANS) are derived from the statistical time that averaged the governing equations. The effect of a turbulent flow is modeled via the Reynolds stresses. Fig. 14 shows the possible combination of computational models and techniques in the modeling of a turbulent flow [92]. The specific flow modeling depends on its turbulence length scale and specific computational techniques to tackle the physics of turbulent flow. Any interface tracking method (ITM) can be straightforwardly combined with the LES model due to its very small resolvable length scale. The combined methods are able to facilitate the interface exchange terms while delivering the time-dependent interfacial kinematics of the model. Moreover, the LES model has become a rather popular and extremely powerful tool in turbulence modeling [93]. In addition, LES is not only limited to the turbulent flow analysis, but it is also applicable for various analyses, such as in aeroacoustics, combustion, gas turbine, and many other engineering areas.

4.3. Post-processing

Post-processing of simulation data is a crucial step to accurately analyze the simulated results and derive accurate conclusions from the CFD models. In addition, it involves the presentation of detailed visualization to describe the physics of the flow and other simulation results to decision-makers. In the CFD analysis of the human upper airway, post-processing is useful to provide flow visualization and for the examination of desired flow properties, such as velocity, pressure, and turbulent Reynolds number. Most post-processing software consist of numerical reporting tool and visualization tool. Numerical reporting tool calculates quantitative

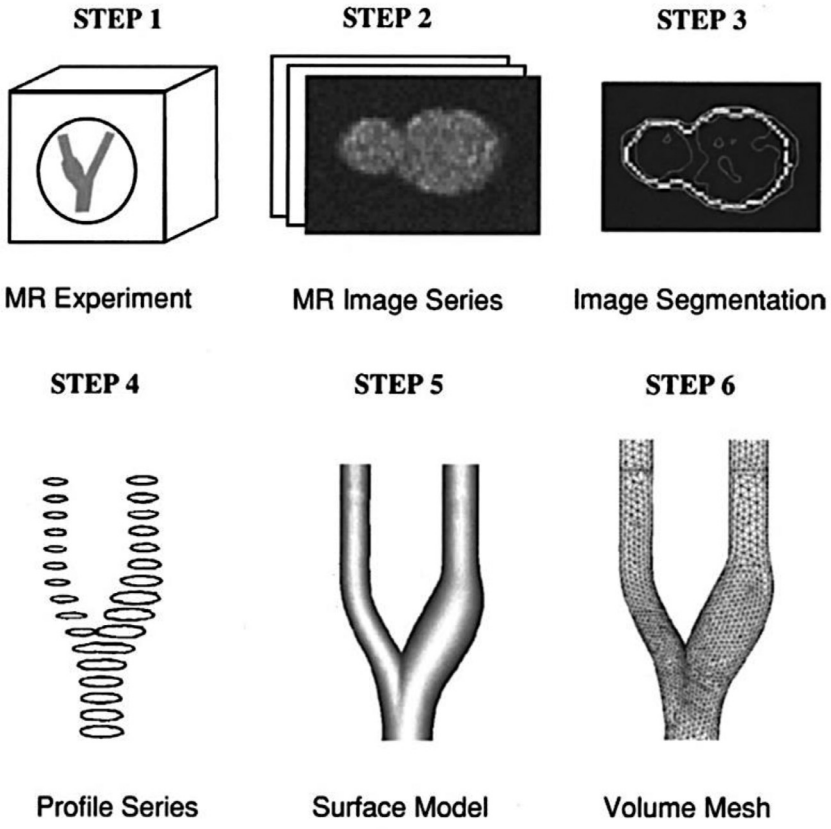

Fig. 12. Construction of an accurate model from MRI images to the volume mesh [74].

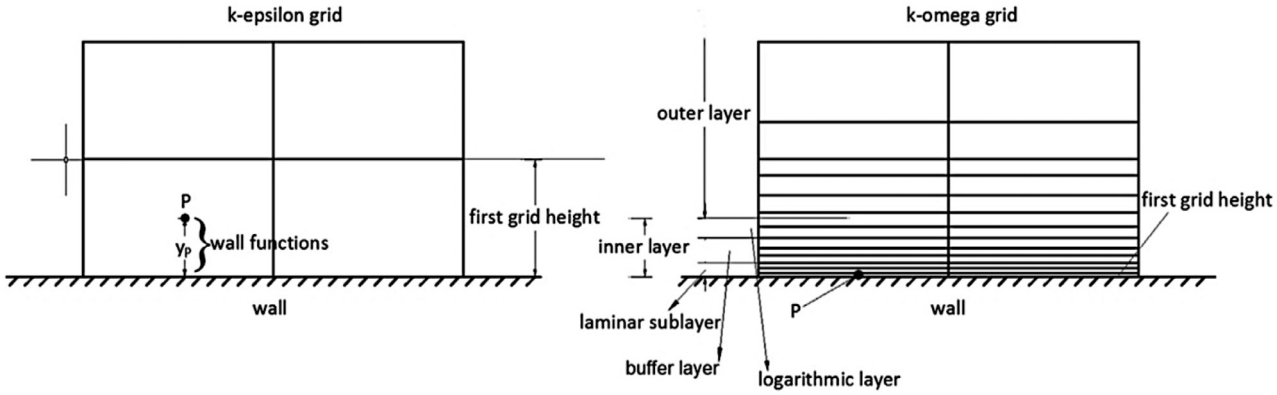

Fig. 13. Comparison of near-wall mesh for k–ε and k–ω models in meshing [83].

results, such as the value of velocity, pressure, temperature, and surface and integrated quantities, among others. Furthermore, the graph of the quantitative results can be plotted via the numerical reporting tool. On the other hand, the visualization tool provides simulation results and extracts the flow properties in various plots, which can be contour plots, vector plots, streamline plots, 2D and 3D surface plots, rendering, et cetera. The animation of flow properties can also be created through the use of the visualization tool. Commonly used commercial software packages for post-processing are ANSYS CFD-Post, Field View, Tecplot 360, and ANSYS EnSight, to name a few. With the aid of these commercial software, revision of model on computational domain, grid size, boundary conditions, setting of the initial conditions and under relaxation factors can easily be done to improve the simulation model and accuracy of results.

5. Characteristics and mechanisms of airway

Literature review on CFD analysis of human upper airway reveals the capability of CFD method in predicting the flow properties and performance of the human upper airway. CFD applications in the study of human upper airway provide a clear visualization of the flow behavior when encountering an obstacle. This information is useful as reference for surgeons and medical practitioners in the treatment of sleep apnea. The literature review also reveals the CFD model of human upper airway that is modeled using the CT scan or MRI. This technique precisely retains the complex geometry, shape, and unique features of the human upper airway for the CFD model in the actual dimension and cross sections. The 3D model created follows the specifications of an actual human upper airway to ensure the anatomical accuracy of the model.

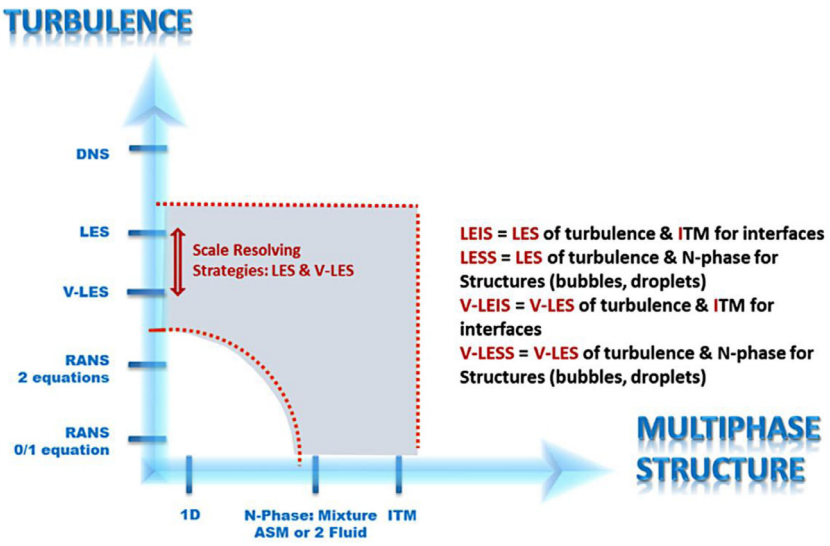

Fig. 14. Possible combinations of computational techniques and models [92].

In early 2006, Xu et al. [94] had developed a model of the upper airway by using the MRI data of three children with OSA. Reynolds-averaged Navier–Stokes equation was applied to simulate the unsteady flow behavior in the upper airway of the child with sleep apnea. They found that the pharyngeal airway shape had crucially affected the internal pressure distribution when compared with nasal resistance. They used this model to explain the regional dynamic airway narrowing phenomenon during the expiration in the upper airway of a child with OSA (Fig. 15). Fig. 15 shows the inspiration pressure, velocity, magnitude, turbulence kinetic energy, and expiration pressure in Caudal and lateral views, and midline sagittal plane. The CFD results demonstrated that the low and negative pressure zones were attributed by the area of restriction, which is related to the cause of sleep apnea.

A CFD approach is only limited to the study of flow aspects. However, in fluid-structure interaction (FSI) approach, CFD integrates with the structure analysis by considering the effect of fluid to the structure deformation and vice-versa. Fluid-structure interaction (FSI) method was used by Dailey and Ghadiali [95] in analyzing the microparticles in deformable pulmonary alveoli. This method was also used by Sun et al. [96] to investigate the soft palate movement and airflow in HUA (Fig. 16). The advantages of FSI are the extended understanding of the overall phenomena for both rigid and flexible regime of the upper airway. The simulation modeling of interaction between the airflow and the soft palate provides a better understanding of the effect of abnormal anatomical airway configuration on the inhale and exhale airflow fields, as well as the displacement of the soft palate. Sun et al. [96] compared both upper airways of healthy persons and obstructive sleep apnea hypopnea syndrome (OSAHS) patients by considering a clinical criterion of the upper airway that is useful for diagnosing the disease.

Jeong et al. [63] carried out a numerical investigation on the aerodynamic force in HUA of patients with OSA using CFD analysis. Their simulation results revealed that the area of restriction in the velopharynx region had induced a turbulent jet flow in the pharyngeal airway. This situation caused higher shear stress and pressure forces surrounding the velopharynx (Fig. 17). In addition, an accurate approach was proposed by Mihai et al. [56] to tackle the airflow situations that occur in the human airway. Steady RANS and LES approaches were applied to the flow modeling. Both modeling approaches yielded different airflow characteristics and static pressure distributions on the human airway walls. The maximum narrowing region of retropalatal pharynx had caused velocity changes and pressure variations in both modeling approaches, as clearly shown in Fig. 17.

CFD approach can provide valuable preliminary information to a surgeon on the geometrical reconstruction of the human upper airway prior to performing the surgery. Sittitavornwong et al. [97] analyzed the anatomical airway changes to predict maxillomandibular advancement (MMA) surgery. They considered a 3D geometrical reconstruction of the airway and investigated the fluid dynamics before and after the surgery using the CFD approach. After the MMA surgery, the dimension of the airway increases, thus reducing the airway resistance and improving the pressure effort of OSAS. The MMA surgery is expected to overcome OSA problems for the patients. Therefore, the study of human airway before and after the MMA surgery becomes a focus in this research area. Moreover, Sittitavornwong et al. [98] extended their research on the effect of changes in soft tissues post-MMA surgery. The dimension of the human airway for OSA patient increases after the MMA surgery (Fig. 18). Pre- and post-surgery results were compared (i.e., pressure distribution and shear stress) in Fig. 19. The comparison study showed a significant improvement in the pressure distribution in the airway. Apart from that, the investigation of mandibular advancement splint (MAS) was reported by Zhao et al. [99] using the fluid-structure interaction method. Chang et al. [100] also used FSI to evaluate the effect before and after the maxillomandibular advancement surgery. In the pre- and post-treatment of OSA, the CFD is a popular approach, in which it can reveal the airflow characteristics and flow variables after the treatment via the unsteady flow analysis. FSI method is considered when displacement and vibration of the soft tissue or membrane such as the trachea are involved. The function of trachea is to regulate the pressure during breathing, coughing, or sneezing. The deformations and stresses of the trachea induced by these ventilation conditions can be computed via the FSI method. Severe muscular membrane deformation leads to critical issue for the physiological function of trachea [101]. Based on the literature review, the capability of FSI method is validated and recognized in various studies. FSI may demonstrate realistic and accurate results on the flow patterns in the study of HUA [106,107]. It is also applicable for the analysis of global and local flow features of the nasal cavity [23].

Recently, the CFD approach has emerged as a virtual surgical concept and reference for medical practitioners and surgeons by providing the simulation analysis [103,104]. The CFD result is used

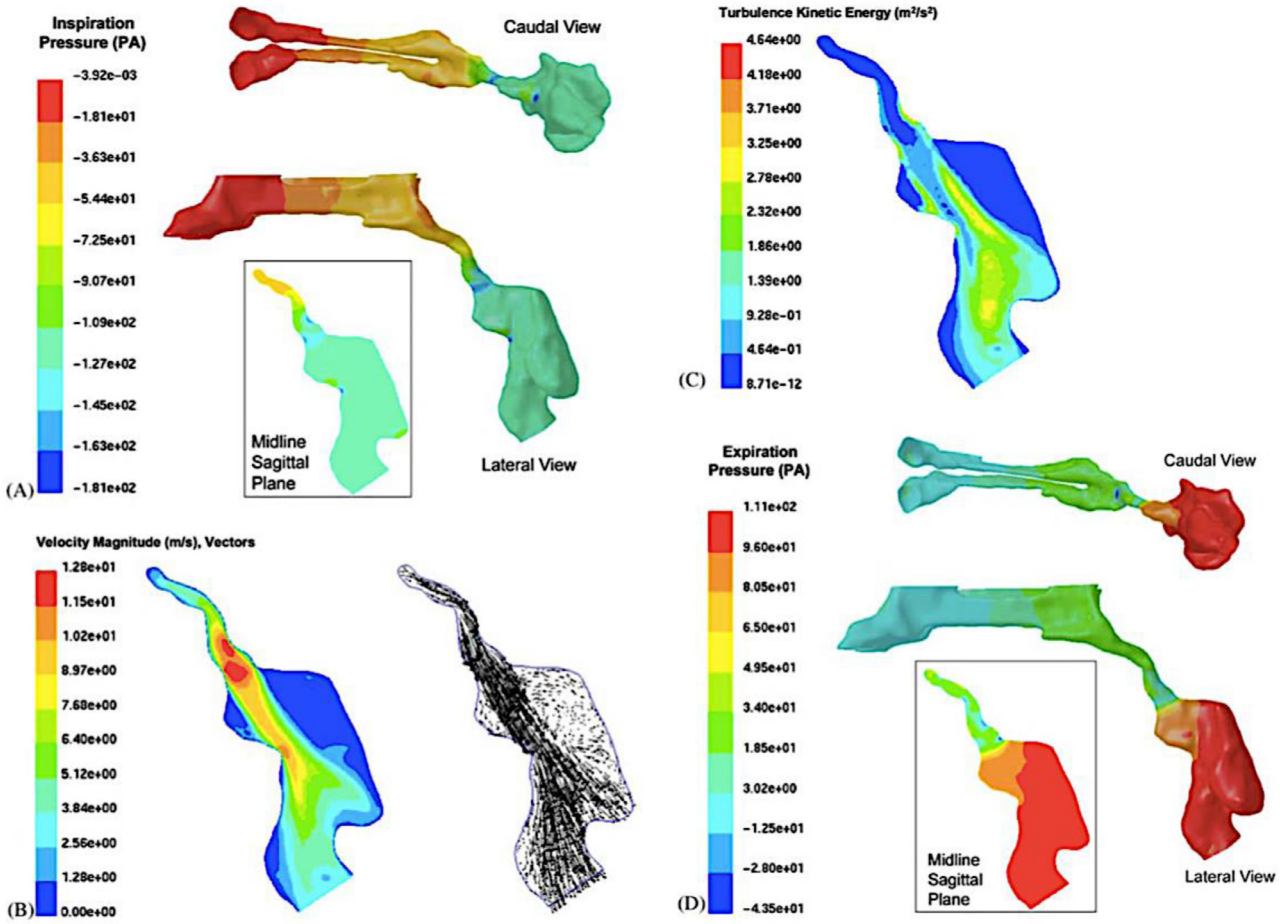

Fig. 15. (A) Pressure contours during inspiration; (B) Velocity magnitude and velocity vector during inspiration; (C) Turbulence kinetic energy; and (D) Pressure contours during expiration [94].

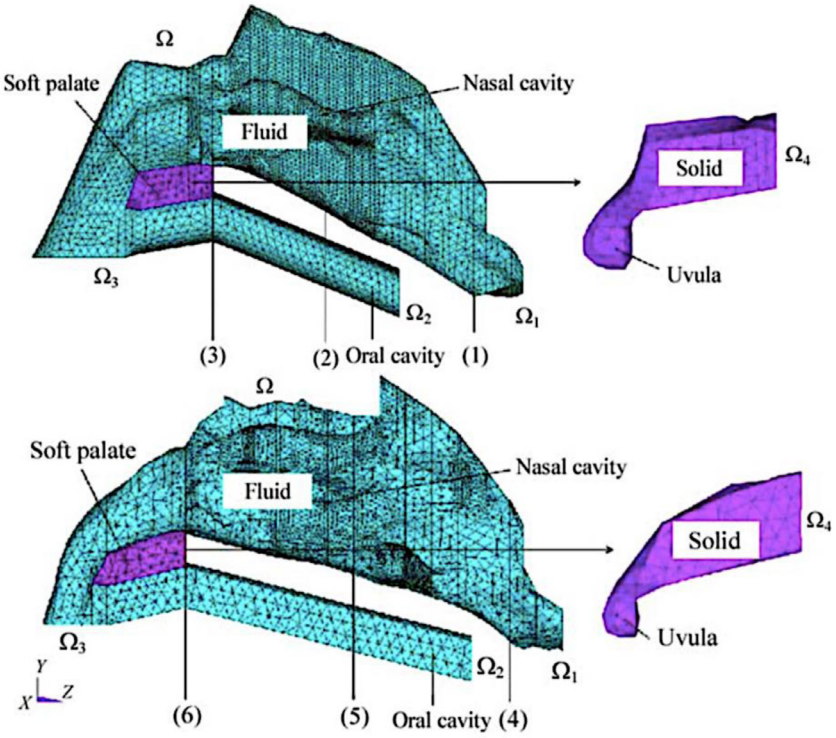

Fig. 16. Fluid-structure interaction (FSI) model. Healthy human upper airway (upper Fig.) and patient with OSAHS (bottom Fig.) [96].

Table 3
Four types of virtual surgery analyses using functional imaging and CFD [105].

Type of surgery	Modifications to baseline (B) airway boundaries on axial scans (baseline and virtual surgeries S1–S4 boundaries are shown in Fig. 19)
S1	Baseline airway boundaries changed on cross-sectional planes A, B, C, and D.
S2	Baseline airway boundaries changed on cross-sectional planes D, E, F, and G.
S3 (= S1 + S2)	Baseline airway boundaries changed on cross-sectional planes A–G. This surgery removes both the constrictions in the airway.
S4 (B < S4 < S2)	Baseline airway boundaries changed on cross-sectional planes D–G. Similar to S2. Airway lumen enlarged compared with the baseline, but not as much as it did in S2.

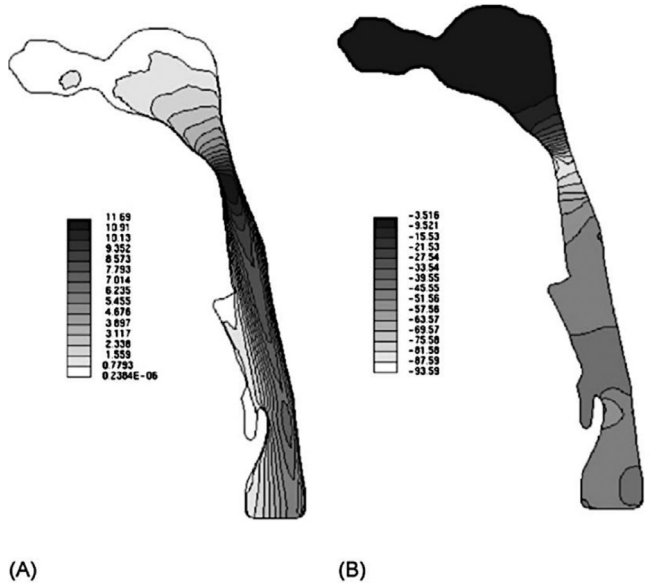

Fig. 17. (A) Midline sagittal plane velocity magnitude; and (B) Pressure contours at midline sagittal plane [63].

for surgical planning and as reference for decision-making procedures in the diseased airways (Table 3). Therefore, the most effective tailored treatment plan can be done by medical personnel to prevent the recurrence of OSA disease. This procedure allows surgeons to modify the airway model, including the geometry reconstruction and boundaries (Fig. 20) based on a certain approach or a series of surgical procedures [105]. In addition, ultra-low-dose computed tomography (CT) scan data were used to predict the treatment outcome on children with sleep-disordered breathing using the CFD approach [106]. The excessive internal pressure forces may lead to the collapse of the upper airway [107], which can be observed in the CFD analysis. The prediction of CFD is consistent with the clinical parameters and data. Thus, it can be a useful tool to evaluate the surgical effects that are associate with OSA problems [108].

Additionally, CFD is used to test and prove the hypothesis model for the treatment of OSA. The CFD model is used to correlate with the treatment response after the adenotonsillectomy surgery (AT) by measuring the apnea-hypopnea index (AHI). A decrease in AHI indicates the success of the hypothesis model in the proposed virtual surgery. CFD, MRI, and physiological data of ten obese children were used to calculate the air pressure and velocity before and after the AT surgery [109]. The correlation between the AT treatment response with other parameters (i.e., pressure-flow ratio, local air pressure drops, geometrical changes, and minimum surface pressure) were considered in the analysis. Moreover, *in vitro* experiment was used to investigate the airflow distribution in the human airway [110]. The numerical and *in vitro* experimental models of airway were reproduced by the CT data, and the experimental model was created by a 3D printer. The particle image velocimetry (PIV) technique was used to measure the velocity and the *in vitro* data were useful for the validation of numerical simulation results. The DNS-LBM model was adopted to assess the flow properties in the upper airway, including the consideration of nasal cavity, pharynx, larynx, and trachea [89].

The CFD approach has been used to quantify the glottis motion, cyclic flow, and its effect towards the respiratory dynamics. Liu et al. [111] had conducted the study of airflow dynamics in an obstructed realistic HUA. The focus was put on the continuous inspiration and expiration with varied respiratory intensities. The above-mentioned authors had proposed a theoretical guidance for the treatment of respiratory diseases. A 3D airway model was developed, with a time-varying glottal aperture. Several aspects, such as vortex topologies, shear stress, flow resistance, and breathing conditions, were considered in their studies. With the aid of

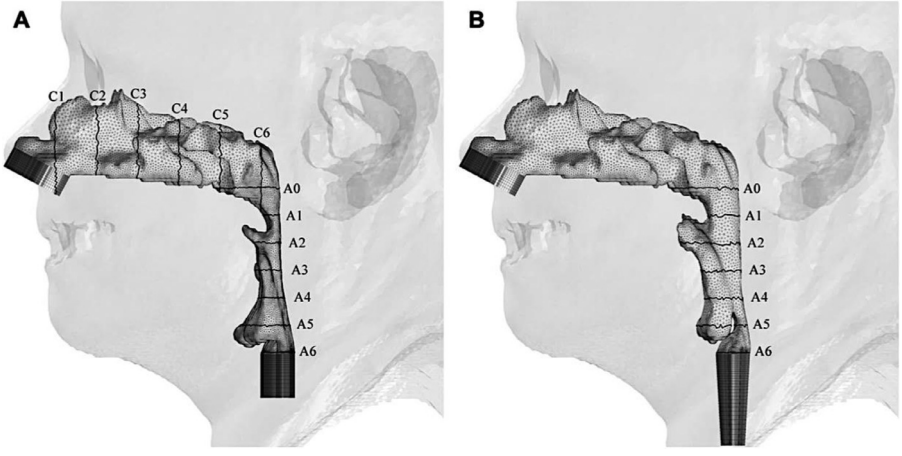

Fig. 18. (A) Pre-surgery and coronal cross sections (C1–C6); (B) Post-surgery of upper airway models and axial cross sections (A0–A6) [98].

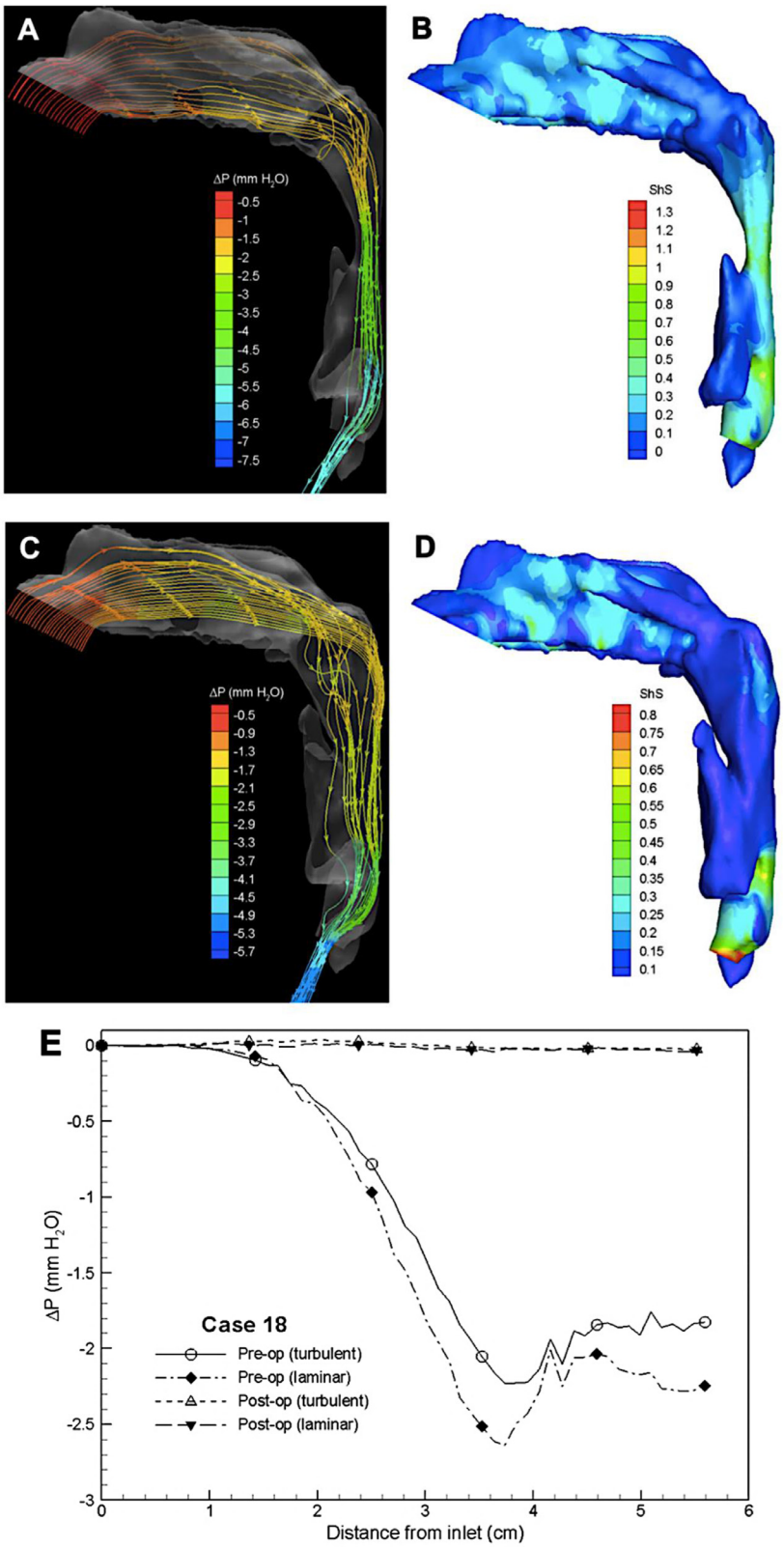

Fig. 19. (A) Preoperative: pressure effort (ΔP) streamlines traces; (B) Preoperative: shear stress (SHS) contours; (C) Postoperative: pressure effort streamlines traces; (D) Postoperative: shear stress contours; and (E) Comparison between preoperative and postoperative pressure distributions along the upper airways [98].

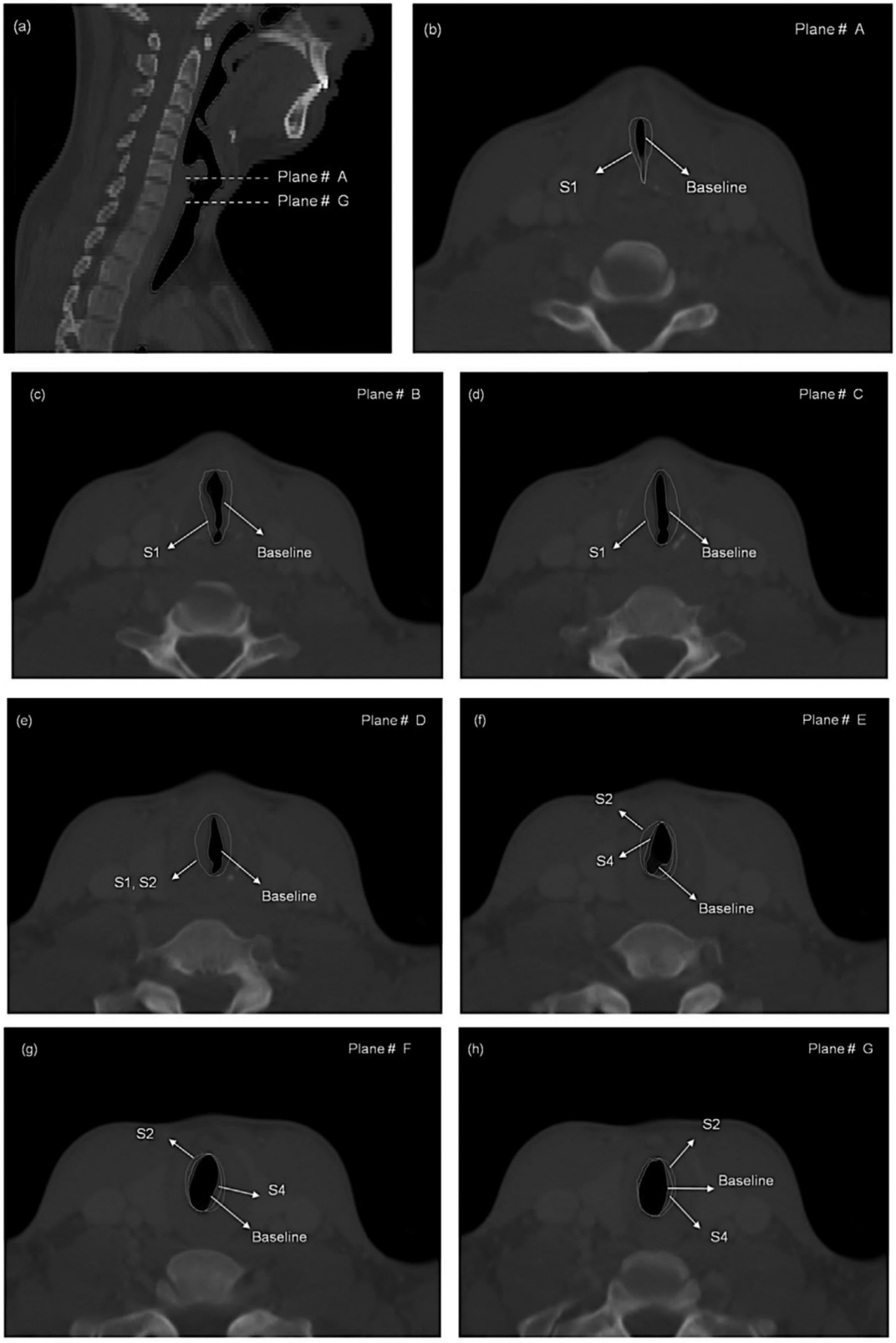

Fig. 20. (a) CT mid-sagittal scan of obstructive region for virtual surgeries; (b)–(h) Axial scans for cross-sectional planes A–G, airway boundaries for virtual surgeries [105].

CFD, the new clinical information can be incorporated into the CFD model to aid in the treatment of tracheomalacia [26]. The passive or active relationship of aerodynamic forces and the airway motion was categorized. Passive relationship indicates the direction of pressure force, and the airway motion is concurrent. The opposite direction for both the pressure force and airway motion is categorized as an active relationship. In heavy breathing and several pathological conditions, the consideration of airway movement is crucial in the simulation analysis. However, FSI models can tackle this airway problem.

Table 4
Latest summary of human airway investigated via CFD. This table summarizes the latest outcome to show the importance of CFD in analyzing human airways that will assist the practitioner perform well.
[The journal is arranged by year, which is from 2018 until the latest publication]

No.	Researcher	Summary of studies
1	Chang et al. [100]	**Software/Solver** SC/Tetra solver (version 12; Software Cradle) was adopted to simulate the airflow. FSI simulations were run using the SC/Tetra Abaqus module (version 12.0; Software Cradle) to assess the flexible region of the airway. **Correlation** The correlation between cross-sectional area after maxillomandibular advancement surgery with pressure, velocity, airway volume, and resistance. **Outcome** Post-MMA surgery, it was learned that there was an increase in airway volume, but a decrease in pressure drop, maximum airflow velocity, and airway resistance for both patients. These results were given by the simulation results of CFD and FSI. FSI simulation portrayed a section of marked airway deformation in both patients prior to the surgery. However, this deformation was considered inconsequential after both patients had undergone the surgery.
2	Liu et al. [102]	**Software/Solver** Fluent 17.2 (ANSYS) was utilized for the computation of the airway flow equations. The ANSYS mechanical simulation software was able to decipher the transient structural equations in the evaluation of the soft tissue deformation and loading. **Correlation** Variation of geometry along the airway with pressure and velocity in determination of location obstruction in upper airway. **Outcome** Identification of areas prone to collapse and precipitate apneic episode was achieved from observation of the tips of the soft palate and the tongue. Consequently, the result was able to rationalize the mechanism of velocity and pressure distribution in the upper airway.
3	Jinxiang et al. [116]	**Software/Solver** ANSYS Fluent (Ansys, Inc.) was used to solve for the mass and momentum conservation equations by taking into account the airway complexity, while the computational meshes were created via the ANSYS ICEM CFD (Ansys, Inc.) **Correlation** The relationship and significance of tidal breathing and glottis motion with regard to the airflow features and energy expenditure in an image-based human upper airway model. **Outcome** Glottis motion on airflow demonstrated aperture and cyclic flow of both altered laryngeal jet instability and vortex generation through main flow speed variations.
4	Alister et al. [26]	**Software/Solver** STAR-CCM+ 11.04.012 was employed in the calculation of Navier–Stokes equations to assess the air pressure and velocity along the domain, which was bounded by moving walls. **Correlation** The researcher investigated the correlation between wall geometry from MRI and airflow (inhale and exhale) in the upper airway. **Outcome** Outcomes of CFD simulations are enhanced through rapid breathing maneuver and integrating the airway movement. There was a 19.8% increase in peak resistance that took place in earlier breath. There was also a 19.2% decrease in overall pressure loss, whereas the proportion of flow in the mouth had elevated by 13.0% in the airway.
5	Vivek at al. [112]	**Software/Solver** Finite volume method (FVM) based on CFD solver (ANSYS Fluent 15) was utilized to computationally simulate the aerosol deposition in the image according to the respiratory tract model. **Correlation** Investigate the correlation between turbulence model and near-wall function. **Outcome** The findings of this work will assist researchers in selecting the optimal range of local Reynolds number (y^+) and turbulence model in simulating the right flow features in a human respiratory system.
6	Yidan et al. [23]	**Software/Solver** The ANSYS Fluent Meshing (ANSYS Inc., Lebanon, NH) was used to mesh the airway model with polyhedral elements. The airflow was assumed to be an incompressible flow (i.e., having constant air density), and a no-slip boundary condition was established at the walls. All simulations were numerically performed via the ANSYS Fluent v17.0 (ANSYS Inc., Lebanon, NH). **Correlation** Determination of the correlation and importance relation between large-to-small conducting airways and inhale mass flow rate (inspiration breathing). **Outcome** The outcome showed that secondary flow currents were observed in the larynx-trachea segment and left main bronchus, whereas the airflow was much smoother with no secondary flow currents for the terminal conducting airway in the right lower lobe.
8	Omid et al. [117]	**Software/Solver** The solid and fluid domains had employed an unstructured mesh, at which it was produced via the ANSA software by BETA CAE Systems USA Inc. Alya high-performance computational mechanics code, a multiphysics code, was also used to solve the FSI problems. **Correlation** Relationship between deformation and collapse of the upper airway when breathing. **Outcome** Findings showed that the sleeping position, gravity, and stiffness of the soft tissues (i.e., utilized in this work as a proxy for neuromuscular effects) were the key aspects of an upper airway collapse.

Recently, the CFD analysis of bifurcation junctions of respiratory tract have been considering the key parameters of the wall turbulence effects, such as local Reynolds number (y^+), wall shear stress (WSS), turbulent energy dissipation (TED), and turbulent kinetic energy (TKE) [112]. Local Reynolds number (y^+) plays a significant role in calculating the wall turbulence and other related parameters. For example, wall shear stress is used as an indicator to determine the wall injury level in the respiratory tract. The upper and lower connecting airways were considered on the respiratory airway tract without omitting it, which extended from the nasal to the terminal bronchioles. Valuable information obtained from the CFD results, such as airflow pattern, can contribute to the baseline data to provide a complete understanding of respiratory physiology [23] and airway collapsibility [113].

Lastly, the CFD applications in simulating the airflow of the upper airway and respiratory are helpful and can be used as a guideline for proposing a surgical approach of the medical treatment to increase the cure rate. It is also beneficial in attaining a better understanding of the mechanism, treatment, and prevention of OSA. Table 4 summarizes the CFD study and comparison of relevant literature in the software and solver used. Wang et al. [114] had also discussed on the relationship between the relation of obstructive sleep apnea and adenotonsillar hypertrophy in children with dissimilar weight status. On the other hand, Vinha et al. [115] had explored the relationship between the dimensions of the palate and pharynx pre- and post-surgery that can affect patients with obstructive sleep apnea.

6. Conclusion

This article presents review on the experimental and numerical method such as, computational fluid dynamics approach, and its application in the analysis of human upper airway (HUA), including the fluid-structure interaction. The experimental study of HUA had utilized the prototype, scale, and *in vitro* models to measure the velocity, pressure, and flow profiles. Nevertheless, limited facilities and measurement devices are some of the constraints in the experimental study. A 3D printing technique was adopted to create the prototype based on the medical images (e.g., MRI and CT scan data), whereby the model was able to retain the actual dimension, geometry, and unique features of the upper airway of each patient. The computational approach is an alternative method used in the HUA research, as it is able to solve the complex phenomena in HUA. Various turbulence models (e.g., RANS, k–ε, k–ω, LES, and DNS) are available in the commercial software to simulate the airflow characteristics and properties. Most studies used commercial software to carry out the CFD analysis on HUA. This is due to the capability of CFD to be integrated with the structural analysis software to perform a fluid-structure interaction simulation in tackling the HUA problems that involve movement, motion, and deformation of soft tissue or airway wall. This work discusses the approach and modeling steps in detail, involving from the preprocessing until post-processing of the model. Solver of turbulence model and model validation are also highlighted in the review. In the modeling of HUA, most studies have converted the medical images into a 3D model via image processing software, such as Mimics software. However, ANSYS is a popular software package for generating the meshing of a model and solving the fluid flow analysis of the HUA. The selection of a solver for the turbulence model is dependent on various scales and combinations of different flow mixtures or phases. Two-equation RANS model (e.g., standard k–ε, SKE, model) is preferred in the simulation study of the HUA. The literature of CFD application in HUA is mostly focused on the fluid dynamic aspects compared with the fluid-structure interaction (FSI). The application of FSI in HUA is still limited in the literature. The study of HUA differs in terms of age (i.e., adult and children), various ventilation conditions (e.g., heavy or light breathing, and inhale or exhale), and region of interest (e.g., geometry parameters, consider the nasal cavity, pharynx, larynx, and trachea). It is reported that the increase in dynamic pressure leads to development of secondary flow. The larynx-trachea segment and left main bronchus is found to be occupied by secondary flow currents. Furthermore, CFD is used to study the airflow characteristics of before and after adenotonsillectomy and maxillomandibular advancement surgeries. Nevertheless, numerous researchers have analyzed the airflow mechanism by exhibiting the velocity, pressure, and shear stress to demonstrate the findings of their work. For example, Navier–Stokes equations are used to provide visualization of the actual mechanism of the airflow. This is because the technique is able to demonstrate meaningful results through its description of the real fluid flow mechanism and via the expression of turbulent kinetic energy (TKE) in their outcomes. Turbulent kinetic energy (TKE) and turbulent energy dissipation (TED) can provide important findings, such as wall shear stress (WSS), to which it can be suggestive of a wall injury, as well as collapsibility tissue of the human upper airway. Additionally, this approach can give the analysis and detect the airway collapse during breathing. The airway collapse is caused by the posterior wall of the trachea bulging forward or tongue collapse during sleep, fully or partly blocking an airway that causes obstruction while exhalation and inspiration. The virtual surgical concept helps surgeons and medical practitioners to plan and determine decision-making procedures in the treatment of diseased airways. In addition, the literature demonstrates that the researchers were able to validate the computational model through clinical and *in vitro* experimental data.

Declaration of Competing Interest

The authors would like to state that there is no conflict of interest whatsoever for this manuscript.

References

[1] P. Nithiarasu, C.-B. Liu, N. Massarotti, Laminar and turbulent flow calculations through a model human upper airway using unstructured meshes, Commun. Numer. Methods Eng. 23 (12) (2006) 1057–1069 Nov., doi:10.1002/cnm.939.
[2] A. Mete, İ.H. Akbudak, Functional anatomy and physiology of airway, Tracheal Intubation (2018) 3–22, doi:10.5772/intechopen.77037.
[3] N.E. Adair, B.L. Matthews, E.F. Haponik, Techniques to assist selection of appropriate therapy for patients with obstructive sleep Apnea, Oper. Tech. Otolaryngol. - Head Neck Surg. 2 (2) (1991) 81–86, doi:10.1016/S1043-1810(10)80202-7.
[4] S.A. Sands, R.L. Owens, A. Malhotra, New approaches to diagnosing sleep-disordered breathing, Sleep Med. Clin. 11 (2) (2016) 143–152, doi:10.1016/j.jsmc.2016.01.005.
[5] J.E. Barrera, Skeletal surgery for obstructive sleep Apnea, Sleep Med. Clin. 13 (4) (2018) 549–558, doi:10.1016/j.jsmc.2018.07.006.
[6] H.C. Lin, M. Friedman, Volumetric tongue reduction for obstructive sleep Apnea, Sleep Med. Clin. 14 (1) (2019) 59–65 no., doi:10.1016/j.jsmc.2018.10.007.
[7] W. Guo, T. Lv, F. She, G. Miao, Y. Liu, R. He, Y. Xue, N.K. Nu, J. Yang, K. Li, P. Zhang, The impact of continuous positive airway pressure on heart rate variability in obstructive sleep Apnea patients during sleep: a meta-analysis, Hear. Lung 47 (5) (2018) 516–524, doi:10.1016/j.hrtlng.2018.05.019.
[8] A. Boudewyns, E. Sforza, M. Zamagni, J. Krieger, Respiratory effort during sleep apneas after interruption of long-term CPAP treatment in patients with obstructive sleep Apnea, Chest 110 (1) (1996) 120–127, doi:10.1378/chest.110.1.120.
[9] K.P. Strohl, J.P. Butler, A. Malhotra, Mechanical properties of the upper airway, Compr. Physiol. 2 (3) (2012) 1853–1872, doi:10.1002/cphy.c110053.
[10] C.P. Wilhelm, R.D. deShazo, S. Tamanna, M.I. Ullah, L.B. Skipworth, The nose, upper airway, and obstructive sleep Apnea, Ann. Allergy Asthma Immunol. 115 (2) (2015) 96–102, doi:10.1016/j.anai.2015.06.011.
[11] J.W. Chen, C.H. Chang, S.J. Wang, Y.T. Chang, C.C. Huang, Submental ultrasound measurement of dynamic tongue base thickness in patients with obstructive sleep Apnea, Ultrasound Med. Biol. 40 (11) (2014) 2590–2598, doi:10.1016/j.ultrasmedbio.2014.06.019.
[12] N. Pombo, N. Garcia, K. Bousson, Classification techniques on computerized systems to predict and/or to detect Apnea: a systematic review, Comput. Methods Programs Biomed. 140 (2017) 265–274, doi:10.1016/j.cmpb.2017.01.001.

[13] M.I. Awad, A. Kacker, Nasal obstruction considerations in sleep Apnea, Otolaryngol. Clin. North Am. 51 (5) (2018) 1003–1009, doi:10.1016/j.otc.2018.05.012.
[14] R.M. Barewal, Obstructive sleep Apnea: the role of gender in prevalence, symptoms, and treatment success, Dental Clin. N. Am. 63 (2) (2019) 297–308, doi:10.1016/j.cden.2018.11.009.
[15] J. Setaro, Obstructive sleep Apnea: a standard of care that works, J. Perianesthesia Nurs. 27 (5) (2012) 323–328, doi:10.1016/j.jopan.2012.06.005.
[16] C. Hardy Tabet, K. Lopez-Bushnell, Sleep, snoring, and surgery: OSA screening matters, J. Perianesthesia Nurs. 33 (6) (2018) 790–800, doi:10.1016/j.jopan.2017.01.009.
[17] H. Chen, G. Aarab, J. de Lange, P. van der Stelt, F. Lobbezoo, The effects of noncontinuous positive airway pressure therapies on the aerodynamic characteristics of the upper airway of obstructive sleep apnea patients: a systematic review, J. Oral Maxillofac. Surg. 76 (7) (2018) pp. 1559.e1-1559.e11, doi:10.1016/j.joms.2018.02.017.
[18] S. Schendel, N. Powell, R. Jacobson, Maxillary, mandibular, and chin advancement: Treatment planning based on airway anatomy in obstructive sleep apnea, J. Oral Maxillofac. Surg. 69 (3) (2011) 663–676, doi:10.1016/j.joms.2010.11.010.
[19] K. Pirklbauer, G. Russmueller, L. Stiebellehner, C. Nell, K. Sinko, G. Millesi, C. Klug, Maxillomandibular advancement for treatment of obstructive sleep apnea syndrome: a systematic review, J. Oral Maxillofac. Surg. 69 (6) (2011), doi:10.1016/j.joms.2011.01.038.
[20] S.C. Leong, X.B. Chen, H.P. Lee, D.Y. Wang, A review of the implications of computational fluid dynamic studies on nasal airflow and physiology, Rhinology 48 (2) (2010) 139–145, doi:10.4193/Rhin09.133.
[21] C.V. Senaratna, J.L. Perret, C.J. Lodge, A.J. Lowe, B.E. Campbell, M.C. Matheson, G.S. Hamilton, S.C. Dharmage, Prevalence of obstructive sleep apnea in the general population: a systematic review, Sleep Med. Rev. 34 (2017) 70–81, doi:10.1016/j.smrv.2016.07.002.
[22] S.B. Kharat, A.B. Deoghare, K.M. Pandey, Development of human airways model for CFD analysis, Mater. Today Proc. 5 (5) (2018) 12920–12926, doi:10.1016/j.matpr.2018.02.277.
[23] Y. Shang, J. Dong, L. Tian, K. Inthavong, J. Tu, Detailed computational analysis of flow dynamics in an extended respiratory airway model, Clin. Biomech. 61 (2019) 105–111 no. July 2018, doi:10.1016/j.clinbiomech.2018.12.006.
[24] A. Khalyfa, A. Gileles-Hillel, D. Gozal, The challenges of precision medicine in obstructive sleep Apnea, Sleep Med. Clin. 11 (2) (2016) 213–226, doi:10.1016/j.jsmc.2016.01.003.
[25] A. Nazareno, C. Newsom, E. Lee, J. Burkard, Obstructive sleep Apnea: emphasis on discharge education after surgery, J. Perianesthesia Nurs. 33 (1) (2018) 28–36, doi:10.1016/j.jopan.2016.08.002.
[26] A.J. Bates, A. Schuh, G. Amine-Eddine, K. McConnell, W. Loew, R.J. Fleck, J.C. Woods, C.L. Dumoulin, R.S. Amin, Assessing the relationship between movement and airflow in the upper airway using computational fluid dynamics with motion determined from magnetic resonance imaging, Clin. Biomech. 66 (2019) 88–96 no. October, doi:10.1016/j.clinbiomech.2017.10.011.
[27] T. Troosters, A. Blondeel, F.M. Rodrigues, W. Janssens, H. Demeyer, Strategies to increase physical activity in chronic respiratory diseases, Clin. Chest Med. 40 (2) (2019) 397–404, doi:10.1016/j.ccm.2019.02.017.
[28] J.W. De Backer, W.G. Vos, A. Devolder, S.L. Verhulst, P. Germonpré, F.L. Wuyts, P.M. Parizel, W. De Backer, Computational fluid dynamics can detect changes in airway resistance in asthmatics after acute bronchodilation, J. Biomech. 41 (1) (2008) 106–113, doi:10.1016/j.jbiomech.2007.07.009.
[29] W. Zhang, Y. Xiang, C. Lu, C. Ou, Q. Deng, Numerical modeling of particle deposition in the conducting airways of asthmatic children, Med. Eng. Phys. 76 (2020) 40–46, doi:10.1016/j.medengphy.2019.10.014.
[30] X.L. Yang, Y. Liu, R.M.C. So, J.M. Yang, The effect of inlet velocity profile on the bifurcation COPD airway flow, Comput. Biol. Med. 36 (2) (2006) 181–194, doi:10.1016/j.compbiomed.2004.11.002.
[31] A. Farghadan, F. Coletti, A. Arzani, Topological analysis of particle transport in lung airways: predicting particle source and destination, Comput. Biol. Med. 115 (2019) 103497, doi:10.1016/j.compbiomed.2019.103497.
[32] J. Xi, J.W. Kim, X.A. Si, R.A. Corley, S. Kabilan, S. Wang, CFD modeling and image analysis of exhaled aerosols due to a growing bronchial tumor: towards non-invasive diagnosis and treatment of respiratory obstructive diseases, Theranostics 5 (5) (2015) 443–455, doi:10.7150/thno.11107.
[33] Q. Gu, S. Qi, Y. Yue, J. Shen, B. Zhang, W. Sun, W. Qian, M.S. Islam, S.C. Saha, J. Wu, Structural and functional alterations of the tracheobronchial tree after left upper pulmonary lobectomy for lung cancer, Biomed. Eng. Online 18 (1) (2019) 1–18, doi:10.1186/s12938-019-0722-6.
[34] L. Chen, X. Zhao, Characterization of air flow and lung function in the pulmonary acinus by fluid-structure interaction in idiopathic interstitial pneumonias, PLoS One 14 (3) (2019) 1–19, doi:10.1371/journal.pone.0214441.
[35] D.M. Kowalczyk, E.T. Hardy, A.F. Lewis, Airway evaluation in obstructive sleep apnea, Oper. Tech. Otolaryngol. - Head Neck Surg. 26 (2) (2015) 59–65, doi:10.1016/j.otot.2015.03.003.
[36] M.A. Slaats, K. Van Hoorenbeeck, A. Van Eyck, W.G. Vos, J.W. De Backer, A. Boudewyns, W. De Backer, S.L. Verhulst, Upper airway imaging in pediatric obstructive sleep apnea syndrome, Sleep Med. Rev. 21 (2015) 59–71, doi:10.1016/j.smrv.2014.08.001.
[37] W. Vos, J. De Backer, A. Devolder, O. Vanderveken, S. Verhulst, R. Salgado, P. Germonpre, B. Partoens, F. Wuyts, P. Parizel, W. De Backer, Correlation between severity of sleep apnea and upper airway morphology based on advanced anatomical and functional imaging, J. Biomech. 40 (10) (2007) 2207–2213, doi:10.1016/j.jbiomech.2006.10.024.
[38] F. Lizal, J. Jedelsky, K. Morgan, K. Bauer, J. Llop, U. Cossio, S. Kassinos, S. Verbanck, J. Ruiz-Cabello, A. Santos, E. Koch, C. Schnabel, Experimental methods for flow and aerosol measurements in human airways and their replicas, Eur. J. Pharm. Sci. 113 (2018) 95–131, doi:10.1016/j.ejps.2017.08.021.
[39] K. Chousangsuntorn, T. Bhongmakapat, N. Apirakkittikul, W. Sungkarat, N. Supakul, J. Laothamatas, Computed tomography characterization and comparison with polysomnography for obstructive sleep Apnea evaluation, J. Oral Maxillofac. Surg. 76 (4) (2018) 854–872, doi:10.1016/j.joms.2017.09.006.
[40] H. Sharafkhaneh, A. Sharafkhaneh, Sleep-related breathing disorders and quality of life, Sleep Med. Clin. 1 (4) (2006) 519–525, doi:10.1016/j.jsmc.2006.10.003.
[41] J. Pirnar, B. Širok, A. Bombač, Effect of airway surface liquid on the forces on the pharyngeal wall: Experimental fluid–structure interaction study, J. Biomech. 63 (2017) 117–124, doi:10.1016/j.jbiomech.2017.08.014.
[42] X.Y. Xu, S.J. Ni, M. Fu, X. Zheng, N. Luo, W.G. Weng, Numerical investigation of airflow, heat transfer and particle deposition for oral breathing in a realistic human upper airway model, J. Therm. Biol. 70 (2017) 53–63, doi:10.1016/j.jtherbio.2017.05.003.
[43] R. Fernández-Parra, P. Pey, L. Zilberstein, M. Malvè, Use of computational fluid dynamics to compare upper airway pressures and airflow resistance in brachycephalic, mesocephalic, and dolichocephalic dogs, Vet. J. 253 (2019) 105392, doi:10.1016/j.tvjl.2019.105392.
[44] S.H. Yeom, J.S. Na, H.D. Jung, H.J. Cho, Y.J. Choi, J.S. Lee, Computational analysis of airflow dynamics for predicting collapsible sites in the upper airways: machine learning approach, J. Appl. Physiol. 127 (4) (2019) 959–973, doi:10.1152/japplphysiol.01033.2018.
[45] R. Piemjaiswang, S. Shiratori, T. Chaiwatanarat, P. Piumsomboon, B. Chalermsinsuwan, Computational fluid dynamics simulation of full breathing cycle for aerosol deposition in trachea: Effect of breathing frequency, J. Taiwan Inst. Chem. Eng. 97 (2019) 66–79, doi:10.1016/j.jtice.2019.02.005.
[46] P.G. Koullapis, P. Hofemeier, J. Sznitman, S.C. Kassinos, An efficient computational fluid-particle dynamics method to predict deposition in a simplified approximation of the deep lung, Eur. J. Pharm. Sci. 113 (2018) 132–144, doi:10.1016/j.ejps.2017.09.016.
[47] T.R. Patel, C. Li, J. Krebs, K. Zhao, P. Malhotra, Modeling congenital nasal pyriform aperture stenosis using computational fluid dynamics, Int. J. Pediatr. Otorhinolaryngol. 109 (2018) 180–184, doi:10.1016/j.ijporl.2018.04.002.
[48] Y. He, A.E. Bayly, A. Hassanpour, Coupling CFD-DEM with dynamic meshing: a new approach for fluid-structure interaction in particle-fluid flows, Powder Technol. 325 (2018) 620–631, doi:10.1016/j.powtec.2017.11.045.
[49] C.F. Adams, P.H. Geoghegan, C.J. Spence, M.C. Jermy, Modelling nasal high flow therapy effects on upper airway resistance and resistive work of breathing, Respir. Physiol. Neurobiol. 254 (2018) 23–29, doi:10.1016/j.resp.2018.03.014.
[50] J. Pirnar, L. Dolenc-Grošelj, I. Fajdiga, I. Žun, Computational fluid-structure interaction simulation of airflow in the human upper airway, J. Biomech. 48 (13) (2015) 3685–3691, doi:10.1016/j.jbiomech.2015.08.017.
[51] J.Y. Tu, M.R. Rasani, K. Inthavong, Simulation of pharyngeal airway interaction with air flow using low-re turbulence model, Model. Simul. Eng. 2011 (2011) no. October 2015, doi:10.1155/2011/510472.
[52] T. Djukic, I. Saveljic, G. Pelosi, O. Parodi, N. Filipovic, Numerical simulation of stent deployment within patient-specific artery and its validation against clinical data, Comput. Methods Programs Biomed. 175 (2019) 121–127, doi:10.1016/j.cmpb.2019.04.005.
[53] F. Raimondi, F. Migliaro, D. De Luca, N. Yousef, J. Rodriguez Fanjul, Clinical data are essential to validate lung ultrasound, Chest 149 (6) (2016) 1575, doi:10.1016/j.chest.2016.02.685.
[54] F. Chouly, A. Van Hirtum, P.Y. Lagrée, X. Pelorson, Y. Payan, Modelling the human pharyngeal airway: validation of numerical simulations using in vitro experiments, Med. Biol. Eng. Comput. 47 (1) (2009) 49–58, doi:10.1007/s11517-008-0412-1.
[55] Y. Zhao, B.B. Lieber, Steady inspiratory flow in a model symmetric bifurcation, J. Biomech. Eng. 116 (4) (1994) 488–496, doi:10.1115/1.2895800.
[56] M. Mihaescu, S. Murugappan, M. Kalra, S. Khosla, E. Gutmark, Large Eddy simulation and Reynolds-Averaged Navier-Stokes modeling of flow in a realistic pharyngeal airway model: an investigation of obstructive sleep Apnea, J. Biomech. 41 (10) (2008) 2279–2288, doi:10.1016/j.jbiomech.2008.04.013.
[57] G. Mylavarapu, S. Murugappan, M. Mihaescu, M. Kalra, S. Khosla, E. Gutmark, Validation of computational fluid dynamics methodology used for human upper airway flow simulations, J. Biomech. 42 (10) (2009) 1553–1559, doi:10.1016/j.jbiomech.2009.03.035.
[58] A.A.T. Borojeni, M.L. Noga, A.R. Martin, W.H. Finlay, Validation of airway resistance models for predicting pressure loss through anatomically realistic conducting airway replicas of adults and children, J. Biomech. 48 (10) (2015) 1988–1996, doi:10.1016/j.jbiomech.2015.03.035.
[59] M. Mihaescu, G. Mylavarapu, E.J. Gutmark, N.B. Powell, Large Eddy simulation of the pharyngeal airflow associated with obstructive sleep Apnea syndrome at pre and post-surgical treatment, J. Biomech. 44 (12) (2011) 2221–2228, doi:10.1016/j.jbiomech.2011.06.006.
[60] V.B. Gawande, A.S. Dhoble, D.B. Zodpe, S. Chamoli, A review of CFD methodology used in literature for predicting thermo-hydraulic performance of a roughened solar air heater, Renew. Sustain. Energy Rev. 54 (2016) 550–605, doi:10.1016/j.rser.2015.10.025.

[61] R. Farré, J.M. Montserrat, D. Navajas, Assessment of upper airway mechanics during sleep, Respir. Physiol. Neurobiol. 163 (1–3) (2008) 74–81, doi:10.1016/j.resp.2008.06.017.

[62] Z. Zhu, C. Zhang, L. Zhang, Experimental and numerical investigation on inspiration and expiration flows in a three-generation human lung airway model at two flow rates, Respir. Physiol. Neurobiol. 262 (2019) 40–48, doi:10.1016/j.resp.2019.01.012.

[63] S.J. Jeong, W.S. Kim, S.J. Sung, Numerical investigation on the flow characteristics and aerodynamic force of the upper airway of patient with obstructive sleep apnea using computational fluid dynamics, Med. Eng. Phys. 29 (6) (2007) 637–651, doi:10.1016/j.medengphy.2006.08.017.

[64] M. Khalili, M. Larsson, B. Müller, Interaction between a simplified soft palate and compressible viscous flow, J. Fluids Struct. 67 (2016) 85–105, doi:10.1016/j.jfluidstructs.2016.09.001.

[65] A.S. Yadav, J.L. Bhagoria, A CFD (computational fluid dynamics) based heat transfer and fluid flow analysis of a solar air heater provided with circular transverse wire rib roughness on the absorber plate, Energy 55 (2013) 1127–1142, doi:10.1016/j.energy.2013.03.066.

[66] F. Lizal, J. Elcner, P.K. Hopke, J. Jedelsky, M. Jicha, Development of a realistic human airway model, Proc. Inst. Mech. Eng. Part H J. Eng. Med. 226 (3) (2012) 197–207, doi:10.1177/0954411911430188.

[67] J.W. De Backer, W.G. Vos, S.L. Verhulst, W. De Backer, Novel imaging techniques using computer methods for the evaluation of the upper airway in patients with sleep-disordered breathing: a comprehensive review, Sleep Med. Rev. 12 (6) (2008) 437–447, doi:10.1016/j.smrv.2008.07.009.

[68] C.D. Bertram, Flow-induced oscillation of collapsed tubes and airway structures, Respir. Physiol. Neurobiol. 163 (1–3) (2008) 256–265, doi:10.1016/j.resp.2008.04.011.

[69] B. Sul, A. Wallqvist, M.J. Morris, J. Reifman, V. Rakesh, A computational study of the respiratory airflow characteristics in normal and obstructed human airways, Comput. Biol. Med. 52 (2014) 130–143, doi:10.1016/j.compbiomed.2014.06.008.

[70] K. Bass, P. Worth Longest, Recommendations for simulating microparticle deposition at conditions similar to the upper airways with two-equation turbulence models, J. Aerosol Sci. 119 (2018) 31–50, doi:10.1016/j.jaerosci.2018.02.007.

[71] H. Mortazavy beni, K. Hassani, S. Khorramymehr, In silico investigation of sneezing in a full real human upper airway using computational fluid dynamics method, Comput. Methods Programs Biomed. 177 (2019) 203–209, doi:10.1016/j.cmpb.2019.05.031.

[72] L.F. Donnelly, Magnetic resonance sleep studies in the evaluation of children with obstructive sleep apnea, Semin. Ultrasound, CT MRI 31 (2) (2010) 107–115, doi:10.1053/j.sult.2009.12.001.

[73] S. Sittitavornwong, P.D. Waite, Imaging the upper airway in patients with sleep disordered breathing, Oral Maxillofac. Surg. Clin. N. Am. 21 (4) (2009) 389–402, doi:10.1016/j.coms.2009.08.004.

[74] D.A. Steinman, Image-based computational fluid dynamics modeling in realistic arterial geometries, Ann. Biomed. Eng. 30 (4) (2002) 483–497, doi:10.1114/1.1467679.

[75] Q. Niu, X. Chi, M.C. Leu, J. Ochoa, Image processing, geometric modeling and data management for development of a virtual bone surgery system, Comput. Aided Surg. 13 (1) (2008) 30–40, doi:10.1080/10929080701882598.

[76] C. Li, J. Jiang, H. Dong, K. Zhao, Computational modeling and validation of human nasal airflow under various breathing conditions, J. Biomech. 64 (2017) 59–68, doi:10.1016/j.jbiomech.2017.08.031.

[77] B.E. Launder, D.B. Spalding, The numerical computation of turbulent flows, Comput. Methods Appl. Mech. Eng. 3 (2) (1974) 269–289 Mar., doi:10.1016/0045-7825(74)90029-2.

[78] T.-H. Shih, W.W. Liou, A. Shabbir, Z. Yang, J. Zhu, A new k-ϵ eddy viscosity model for high reynolds number turbulent flows, Comput. Fluids 24 (3) (1995) 227–238 Mar., doi:10.1016/0045-7930(94)00032-T.

[79] W. D.C., Turbulent modeling for CFD, DCW Ind. Inc. (2004).

[80] F.R. Menter, Two-equation eddy-viscosity turbulence models for engineering applications, AIAA J 32 (8) (1994) 1598–1605, doi:10.2514/3.12149.

[81] F.R. Menter, R.B. Langtry, S.R. Likki, Y.B. Suzen, P.G. Huang, S. Völker, A correlation-based transition model using local variables - Part I: model formulation, J. Turbomach. 128 (3) (2006) 413–422, doi:10.1115/1.2184352.

[82] R.B. Langtry, F.R. Menter, S.R. Likki, Y.B. Suzen, P.G. Huang, S. Völker, A correlation-based transition model using local variables - Part II: test cases and industrial applications, J. Turbomach. 128 (3) (2006) 423–434, doi:10.1115/1.2184353.

[83] D. Mohotti, K. Wijesooriya, D. Dias-da-Costa, Comparison of Reynolds averaging Navier-Stokes (RANS) turbulent models in predicting wind pressure on tall buildings, J. Build. Eng. 21 (2019) 1–17 August 2018, doi:10.1016/j.jobe.2018.09.021.

[84] D. Modesti, S. Pirozzoli, F. Grasso, Direct numerical simulation of developed compressible flow in square ducts, Int. J. Heat Fluid Flow 76 (2019) 130–140 January, doi:10.1016/j.ijheatfluidflow.2019.02.002.

[85] A. Orazzo, S. Tanguy, Direct numerical simulations of droplet condensation, Int. J. Heat Mass Transf. 129 (2019) 432–448, doi:10.1016/j.ijheatmasstransfer.2018.07.094.

[86] R. Taherinezhad, G. Zarepour, Evaluation of pressure oscillations by a laboratory motor, Chinese J. Aeronaut. (2020) January, doi:10.1016/j.cja.2019.11.010.

[87] H. Zhu, H. Zhao, T. Zhou, Direct numerical simulation of flow over a slotted cylinder at low Reynolds number, Appl. Ocean Res. 87 (2019) 9–25 January, doi:10.1016/j.apor.2019.01.019.

[88] D. Angeli, E. Stalio, A fast algorithm for direct numerical simulation of turbulent convection with immersed boundaries, Comput. Fluids 183 (2019) 148–159, doi:10.1016/j.compfluid.2019.03.002.

[89] Y. Wang, S. Elghobashi, On locating the obstruction in the upper airway via numerical simulation, Respir. Physiol. Neurobiol. 193 (1) (2014) 1–10, doi:10.1016/j.resp.2013.12.009.

[90] J. Ruiz, A.S. Kaiser, B. Zamora, C.G. Cutillas, M. Lucas, CFD analysis of drift eliminators using RANS and LES turbulent models, Appl. Therm. Eng. 105 (2016) 979–987, doi:10.1016/j.applthermaleng.2016.01.108.

[91] R. Bouffanais, Advances and challenges of applied large-eddy simulation, Comput. Fluids 39 (5) (2010) 735–738, doi:10.1016/j.compfluid.2009.12.003.

[92] D. Lakehal, Status and future developments of Large-Eddy Simulation of turbulent multi-fluid flows (LEIS and LESS), Int. J. Multiph. Flow 104 (2018) 322–337, doi:10.1016/j.ijmultiphaseflow.2018.02.018.

[93] Y. Zhiyin, Large-eddy simulation: past, present and the future, Chinese J. Aeronaut. 28 (1) (2015) 11–24, doi:10.1016/j.cja.2014.12.007.

[94] C. Xu, S.H. Sin, J.M. McDonough, J.K. Udupa, A. Guez, R. Arens, D.M. Wootton, Computational fluid dynamics modeling of the upper airway of children with obstructive sleep apnea syndrome in steady flow, J. Biomech. 39 (11) (2006) 2043–2054, doi:10.1016/j.jbiomech.2005.06.021.

[95] H.L. Dailey, S.N. Ghadiali, Fluid-structure analysis of microparticle transport in deformable pulmonary alveoli, J. Aerosol Sci. 38 (3) (2007) 269–288, doi:10.1016/j.jaerosci.2007.01.001.

[96] X. Sun, C. Yu, Y. Wang, Y. Liu, Numerical simulation of soft palate movement and airflow in human upper airway by fluid-structure interaction method, Acta Mech. Sin. Xuebao 23 (4) (2007) 359–367, doi:10.1007/s10409-007-0083-4.

[97] S. Sittitavornwong, P.D. Waite, A.M. Shih, R. Koomullil, Y. Ito, G.C. Cheng, D. Wang, Evaluation of obstructive sleep Apnea syndrome by computational fluid dynamics, Semin. Orthod. 15 (2) (2009) 105–131, doi:10.1053/j.sodo.2009.01.005.

[98] S. Sittitavornwong, P.D. Waite, A.M. Shih, G.C. Cheng, R. Koomullil, Y. Ito, J.K. Cure, S.M. Harding, M. Litaker, Computational fluid dynamic analysis of the posterior airway space after maxillomandibular advancement for obstructive sleep apnea syndrome, J. Oral Maxillofac. Surg. 71 (8) (2013) 1397–1405, doi:10.1016/j.joms.2013.02.022.

[99] M. Zhao, T. Barber, P.A. Cistulli, K. Sutherland, G. Rosengarten, Simulation of upper airway occlusion without and with mandibular advancement in obstructive sleep apnea using fluid-structure interaction, J. Biomech. 46 (15) (2013) 2586–2592, doi:10.1016/j.jbiomech.2013.08.010.

[100] K.K. Chang, K.B. Kim, M.W. McQuilling, R. Movahed, Fluid structure interaction simulations of the upper airway in obstructive sleep apnea patients before and after maxillomandibular advancement surgery, Am. J. Orthod. Dentofac. Orthop. 153 (6) (2018) 895–904, doi:10.1016/j.ajodo.2017.08.027.

[101] M. Malvè, A. Pérez del Palomar, O. Trabelsi, J.L. López-Villalobos, A. Ginel, M. Doblaré, Modeling of the fluid structure interaction of a human trachea under different ventilation conditions, Int. Commun. Heat Mass Transf. 38 (1) (2011) 10–15, doi:10.1016/j.icheatmasstransfer.2010.09.010.

[102] Y. Liu, J. Mitchell, Y. Chen, W. Yim, W. Chu, R.C. Wang, Study of the upper airway of obstructive sleep apnea patient using fluid structure interaction, Respir. Physiol. Neurobiol. 249 (2018) 54–61 no. May, doi:10.1016/j.resp.2018.01.005.

[103] Z. Zheng, H. Liu, Q. Xu, W. Wu, L. Du, H. Chen, Y. Zhang, D. Liu, Computational fluid dynamics simulation of the upper airway response to large incisor retraction in adult class I bimaxillary protrusion patients, Sci. Rep. 7 (1) (May 2017) 45706, doi:10.1038/srep45706.

[104] W.M. Faizal, N.N.N. Ghazali, I.A. Badruddin, M.Z. Zainon, A.A. Yazid, M.A. Bin Ali, C.Y. Khor, N.B. Ibrahim, R.M. Razi, A review of fluid-structure interaction simulation for patients with sleep related breathing disorders with obstructive sleep, Comput. Methods Programs Biomed. 180 (Oct. 2019) 105036, doi:10.1016/j.cmpb.2019.105036.

[105] G. Mylavarapu, M. Mihaescu, L. Fuchs, G. Papatziamos, E. Gutmark, Planning human upper airway surgery using computational fluid dynamics, J. Biomech. 46 (12) (2013) 1979–1986, doi:10.1016/j.jbiomech.2013.06.016.

[106] C. Van Holsbeke, W. Vos, K. Van Hoorenbeeck, A. Boudewyns, R. Salgado, P.R. Verdonck, J. Ramet, J. De Backer, W. De Backer, S.L. Verhulst, Functional respiratory imaging as a tool to assess upper airway patency in children with obstructive sleep apnea, Sleep Med 14 (5) (2013) 433–439, doi:10.1016/j.sleep.2012.12.005.

[107] M. Zhao, T. Barber, P. Cistulli, K. Sutherland, G. Rosengarten, Computational fluid dynamics for the assessment of upper airway response to oral appliance treatment in obstructive sleep apnea, J. Biomech. 46 (1) (2013) 142–150, doi:10.1016/j.jbiomech.2012.10.033.

[108] M.Z. Lu, Y. Liu, J.Y. Ye, H.Y. Luo, Large Eddy Simulation of flow in realistic human upper airways with obstructive sleep, Procedia Comput. Sci. 29 (2014) 557–564, doi:10.1016/j.procs.2014.05.050.

[109] H. Luo, S. Sin, J.M. McDonough, C.R. Isasi, R. Arens, D.M. Wootton, Computational fluid dynamics endpoints for assessment of adenotonsillectomy outcome in obese children with obstructive sleep apnea syndrome, J. Biomech. 47 (10) (2014) 2498–2503, doi:10.1016/j.jbiomech.2014.03.023.

[110] N.L. Phuong, K. Ito, Investigation of flow pattern in upper human airway including oral and nasal inhalation by PIV and CFD, Build. Environ. 94 (2015) 504–515, doi:10.1016/j.buildenv.2015.10.002.

[111] X. Liu, W. Yan, Y. Liu, Y.S. Choy, Y. Wei, Numerical investigation of flow characteristics in the obstructed realistic human upper airway, Comput. Math. Methods Med. (2016) no. 2008, 2016, doi:10.1155/2016/3181654.

[112] V.K. Srivastav, A.R. Paul, A. Jain, Capturing the wall turbulence in CFD simulation of human respiratory tract, Math. Comput. Simul. 160 (2019) 23–38, doi:10.1016/j.matcom.2018.11.019.
[113] L. Zhu, H. Liu, Z. Fu, J. Yin, Computational fluid dynamics analysis of H-uvulopalatopharyngoplasty in obstructive sleep apnea syndrome, Am. J. Otolaryngol. 40 (2) (2019) 197–204 Mar., doi:10.1016/j.amjoto.2018.12.001.
[114] J. Wang, Y. Zhao, W. Yang, T. Shen, P. Xue, X. Yan, D. Chen, Y. Qiao, M. Chen, R. Ren, J. Ren, Y. Xu, Y. Zheng, J. Zou, X. Tang, Correlations between obstructive sleep apnea and adenotonsillar hypertrophy in children of different weight status, Sci. Rep. 9 (1) (2019) 1–7, doi:10.1038/s41598-019-47596-5.
[115] P.P. Vinha, E.R. Thuler, F.V. de Mello-Filho, Effects of surgically assisted rapid maxillary expansion on the modification of the pharynx and hard palate and on obstructive sleep apnea, and their correlations, J. Cranio-Maxillofac. Surg. 48 (4) (2020) 339–348, doi:10.1016/j.jcms.2020.02.007.
[116] J. Xi, X. April Si, H. Dong, H. Zhong, Effects of glottis motion on airflow and energy expenditure in a human upper airway model, Eur. J. Mech. B/Fluids 72 (2018) 23–37, doi:10.1016/j.euromechflu.2018.04.011.
[117] O. Bafkar, J.C. Cajas, H. Calmet, G. Houzeaux, G. Rosengarten, D. Lester, V. Nguyen, S. Gulizia, I.S. Cole, Impact of sleeping position, gravitational force & effective tissue stiffness on obstructive sleep apnoea, J. Biomech. (2020) 109715, doi:10.1016/j.jbiomech.2020.109715.